

REPORT
ON
THE COOPERATIVE STUDY PROJECT
ON THE DEEPSEA MINERAL RESOURCES
IN SELECTED OFFSHORE AREAS OF THE SOPAC REGION

(VOLUME 1)

SEA AREA OF THE KINGDOM OF TONGA

March 1996

JICA LIBRARY

J 1127750(6)

JAPAN INTERNATIONAL COOPERATION AGENCY
METAL MINING AGENCY OF JAPAN

MPN
CR(1)
96-055

RY

**REPORT
ON
THE COOPERATIVE STUDY PROJECT
ON THE DEEPSEA MINERAL RESOURCES
IN SELECTED OFFSHORE AREAS OF THE SOPAC REGION**

(VOLUME 1)

SEA AREA OF THE KINGDOM OF TONGA

March 1996

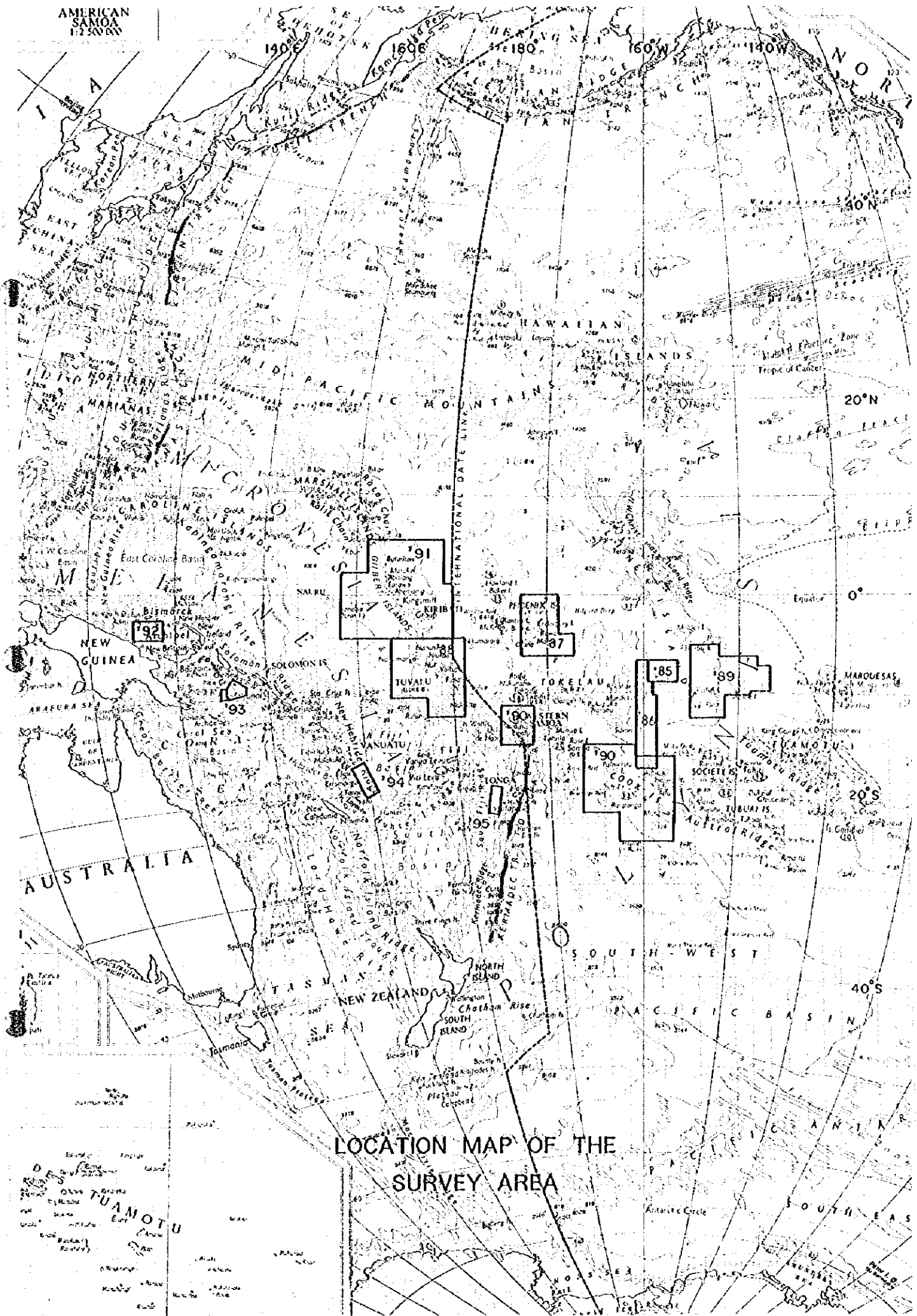
**JAPAN INTERNATIONAL COOPERATION AGENCY
METAL MINING AGENCY OF JAPAN**



1127750(6)

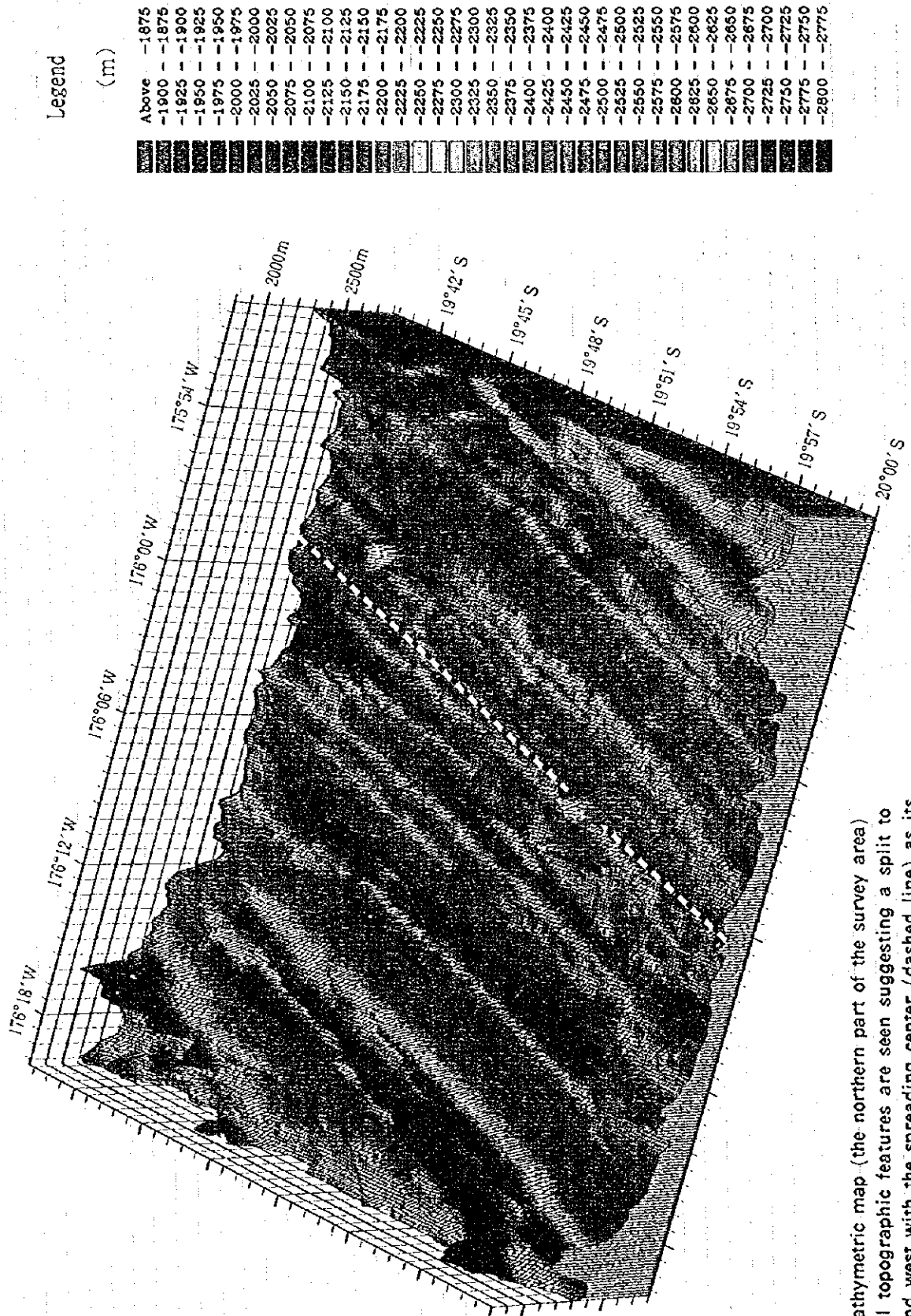


AMERICAN
SAMOA
1:250,000



LOCATION MAP OF THE
SURVEY AREA

DETAILED MAP OF
TUAMOTU



3-D bathymetric map (the northern part of the survey area)
 Several topographic features are seen suggesting a split to east and west with the spreading center (dashed line) as its center.

PREFACE

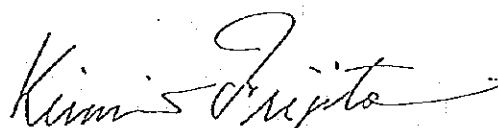
In response to a request by the South Pacific Applied Geoscience Commission (SOPAC), the Government of Japan has undertaken the studies relating to mineral prospecting to assess mineral resources potential in the deep sea bottom of the offshore regions of SOPAC member countries. Implementation of the survey has been consigned to Japan International Cooperation Agency (JICA). JICA, considering the technical nature of the geological and mineral prospecting studies, entrusted the studies to the Metal Mining Agency of Japan (MMAJ).

The survey has been undertaken for a five year period starting from fiscal 1995. The first year of the survey was carried out within the exclusive economic zone of the Kingdom of Tonga. MMAJ dispatched the Hakurei Maru No.2, a research vessel for investigating mineral resources in the deep sea bottom, to the sites for total 69 days, from July 2, 1995 to September 8, 1995, successfully completing the survey on schedule with the cooperation of the Kingdom of Tonga.

This report sums up the results of the first year survey.

We wish to extend our sincere thanks to all persons concerned, especially for the cooperation rendered to us by the Secretariat of SOPAC, the Government of the Kingdom of Tonga as well as the Ministry of Foreign Affairs, the Ministry of International Trade and Industry, and the Japanese Embassy in the Republic of Fiji.

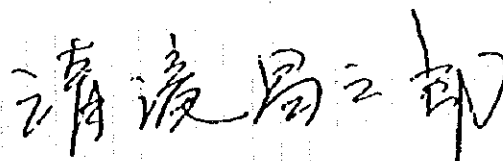
March, 1996.



Kimio FUJITA

President

Japan International Cooperation Agency



Shozaburo KIYOTAKI

President

Metal Mining Agency of Japan

ABSTRACT

The third phase of the cooperative study project on the deepsea mineral resources for SOPAC member countries began at 1995 and runs for five years. This first year survey was carried out in the sea area within an exclusive economic zone of the Kingdom of Tonga, which locates in the middle east of Lau Basin and has an area of about 36,000 km². The survey period on site was 69 days from July 2 to September 8. The target of mineral resources was hydrothermal ore deposits.

The former half of the survey (Leg 1) is regarded as a regional survey, aiming mainly at making a bathymetric map by bathymetric survey with track lines of 2 nautical miles intervals in parallel. At the same time, the magnetic survey was also carried out to help the geological interpretation.

The latter half of the survey (Leg 2) is a detailed survey. The target area for the detailed investigation was selected on the basis of the results of the bathymetric and magnetic surveys. First, sea floor observation by Finder attached Deepsea Camera system (FDC) was carried out, and in a restricted area the Side Scan Sonar (SSS) survey was carried out to study the precise topography and sea floor conditions. Then, the samplings of rocks and sediments were carried out mainly in the spreading center running near north-south direction in the central part of the survey area, where the latest volcanic activities occur in the Lau Basin.

As a result of bathymetric survey, in the central part of the survey area, seafloor spreading center developing in NNE-SSW trending was observed and its topographic shape was clarified, suggesting some tectonic movements. In addition, continuous spreading center running from the southern part of the survey area, which consists of several grabens and ridges, and overlapping spreading center were in the central part of the area also observed.

Acoustic reflection image drawn up using sound pressure received by MBES clearly indicates the shape of spreading center as strong reflector. This image has been useful results for sea floor conditions such as distribution of sediments as well as selection of FDC survey area.

As a result of magnetic survey, magnetic anomaly is generally not so strong, however, NNE-SSW trending magnetic anomaly zone was observed along the general trend of the area. According to magnetization analysis, continuous high magnetization belts were detected in the southern to the central part of the area and arrangements of high magnetization were detected in the northern part. These were considered to be caused by the spreading movements. Furthermore, from the characteristics of distribution of positive magnetization dominant area in the northern and the southern parts of the area, it was estimated that spreading rate increase towards north or beginning age of spreading may be earlier in the northern part than in the southern part.

As an ore deposits investigation, sea floor observation by FDC was first carried out to study the features of sea floor sediments and geological structures, and the SSS was used for a supplementary survey. On the basis of these results, samplings were carried out by using Large Corer (LC), Finner attached Power Grab (FPG) and Chain Bucket dredge (CB). The sampling area was focused to the spreading center where younger volcanic rocks distribute.

The results of SSS survey show a lot of fault structure, some uplifts in a mound shape and records like a plume which is a direct indication of hydrothermal activities. In the sea floor observations by FDC, however, only precipitations of manganese and iron oxides were locally observed at some places and neither hydrothermal ore deposit nor its indication was found out.

Basalt lava and sediments were collected by samplings, but no ore indication such as alteration, which is characteristic to hydrothermal ore deposit, was observed.

The survey area includes almost all the Valu Fa Ridge, which is a current spreading center, and is expected to have ore deposits. In this investigation, however, hydrothermal activity, hydrothermal ore deposits and their significant indications were not observed at all. This reason is presumed that the cap rock sealing the hydrothermal activity has not been formed because the hydrothermal activity has been weak and not been continuous. Judging from the results of this investigation and the past investigations around the survey area, it is concluded that the potential of ore deposits is low in the northern part of the survey area and high in the spreading ridge of the southern part.

CONTENTS

	Page
PHOTOGRAVURE	
PREFACE	
ABSTRACT	
CHAPTER 1 OUTLINE OF THE SURVEY	1
1-1 Survey Title	1
1-2 Purpose of the Survey	1
1-3 The Survey Area	1
1-4 Survey Period	1
1-5 Participants of the Survey	3
1-6 Apparatus and Equipment for the Survey	4
1-7 Schedule of the Survey Cruise	4
CHAPTER 2 SURVEY METHOD	11
2-1 Survey Plan	11
2-2 Numbering	11
2-3 Ship Positioning and Positions of Towed Fish	13
2-4 Acoustic Sounding	14
2-5 Magnetic Survey	14
2-6 Seafloor Observation and Photographing	14
2-7 Sampling	14
2-8 Sea Water Survey (CTD Measurement)	16
2-9 Data Processing and Analysis	16
CHAPTER 3 BATHYMETRY AND GEOLOGICAL STRUCTURE	18
3-1 Tectonic Setting around the Survey Area	18
3-2 Bathymetry	19
3-3 Magnetic Survey	23
(1) Total Magnetic Force	23
(2) Magnetic Anomaly	25
(3) Reduction-to-the-pole Anomaly	28

(4) Magnetization	30
(5) Magnetic Structure	32
3-4 Geological Structure	34
(1) Geological Structure	34
(2) MBES Acoustic Reflection Image	39
(3) nSBP Survey	41
CHAPTER 4 ORE DEPOSITS INVESTIGATION	47
4-1 General	47
4-2 SSS Survey	53
4-3 FDC Survey	57
4-4 Sampling	67
(1) LC	67
(2) FPG	71
(3) CB	74
4-5 Survey Results	77
(1) Geology and Rock Facies	77
(2) Muddy Sediments	79
(3) Ore Indications	80
(4) Temperature Anomalies	82
CHAPTER 5 RESULTS OF CHEMICAL ANALYSIS AND OBSERVATIONS	87
5-1 Microscopic Observation of Thin Section	87
5-2 Microscopic Observation of Polish	91
5-3 X-ray Diffraction Analysis	91
5-4 Dating the Rock	91
5-5 Chemical Analysis of Rocks	96
5-6 Chemical Analysis of Sea Floor Sediments	107
5-7 Microfossil in Sea Floor Sediments	121
CHAPTER 6 DISCUSSION	127
CHAPTER 7 CONCLUSION	129

[References]

[APPENDIX]

Table 1	Results of FDC survey
Table 2(1),(2)	Results of sampling survey
Table 3	Ore indications
Table 4(1)-(4)	Sample list of analysis and observation
Table 5	Sea-water sound velocity for MBES
Table 6	Weather and sea-state data
Fig. 1	Bathymetric profiles (all lines)
Fig. 2	MBES Track line map
Fig. 3	PGM Track line map
Fig. 4	SSS Vehicle position map
Fig. 5(1)-(13)	Route-maps of FDC observation
Fig. 6(1)-(3)	Columnar charts of LC core
Fig. 7	3-D bathymetric map based on MBES

[List of Inserted Figures]

Fig. 1-3-1	Location map of survey area	2
Fig. 1-6-1(1)-(3)	Photographs of survey equipments	6
Fig. 2-1-1	Survey planning map	12
Fig. 2-4-1	Location map of track line	15
Fig. 2-9-1	Data analysis and processing flowsheet	17
Fig. 3-1-1	Tectonic setting map around the survey area	18
Fig. 3-2-1	Color-coded bathymetric map based on MBES	20
Fig. 3-2-2	Bathymetric map based on MBES	21
Fig. 3-2-3	Bathymetric profiles	22
Fig. 3-3-1	Total magnetic force map	24
Fig. 3-3-2	Magnetic anomaly map from IGRF residual	26
Fig. 3-3-3	Magnetic anomaly map from trend surface residual	27
Fig. 3-3-4	Reduction-to-the-pole anomaly map	29
Fig. 3-3-5	Magnetization amplitude map	31
Fig. 3-3-6	Magnetic structural map	33
Fig. 3-4-1	Lineament map	35
Fig. 3-4-2	Geological structure map	37
Fig. 3-4-3	Acoustic reflection image based on MBES	40
Fig. 3-4-4	Distribution map of nSBP type	43
Fig. 3-4-5	Typical records for each type	45
Fig. 4-1-1	Area map of location maps of ore deposits investigation	48
Fig. 4-1-2(1)-(4)	Location map of ore deposits investigation	49
Fig. 4-2-1(1)-(3)	Results of side scan sonar survey	54
Fig. 4-3-1(1)-(4)	Photographs of FDC observation	58
Fig. 4-4-1(1),(2)	Photographs of LC sampling	68
Fig. 4-4-2	Photographs of FPG sampling	72
Fig. 4-4-3	Photographs of CB sampling	75
Fig. 4-5-1(1)-(3)	Temperature and CTD depth profile	84
Fig. 5-1-1(1),(2)	Photographs of microscopic observation of thin section	89
Fig. 5-2-1	Photographs of microscopic observation of polish	93
Fig. 5-5-1	AFM diagram	102
Fig. 5-5-2	MnO-TiO ₂ -P ₂ O ₅ diagram	103
Fig. 5-5-3	Zr-Nb-Y diagram	104
Fig. 5-5-4	SiO ₂ -K ₂ O variation diagram	104
Fig. 5-5-5	REE normalized pattern diagram to chondrite	105
Fig. 5-6-1(1)-(3)	Bar graphs of chemical analysis data of sea floor sediments	118
Fig. 5-7-1(1),(2)	Photographs of microscopic observation of microfossils	123

[List of Inserted Tables]

Table 1-6-1	Survey apparatus and equipment	5
Table 1-7-1	Survey achievements	9
Table 1-7-2	Records of survey schedule	10
Table 4-5-1	List of temperature anomalies	83
Table 5-1-1	Results of microscopic observation of thin section	88
Table 5-2-1	Results of microscopic observation of polish	92
Table 5-3-1	Results of X-ray diffraction analysis	92
Table 5-4-1	Results of age determination analysis	94
Table 5-5-1	Analytical components	97
Table 5-5-2	Analytical components and sample No.	97
Table 5-5-3(1)-(3)	Results of chemical analysis of rocks	98
Table 5-6-1(1)-(4)	Results of chemical analysis of sea floor sediments	108
Table 5-6-2	Basic statistics	113
Table 5-6-3	Correlation coefficient	114
Table 5-6-4	Results of factor analysis	115
Table 5-7-1	Results of microscopic observation of microfossils	122

CHAPTER 1 OUTLINE OF THE SURVEY

1-1 Survey Title

"The Cooperative Study Project on the Deepsea Mineral Resources
in the Sea Area of the Kingdom of Tonga"

1-2 Purpose of the Survey

The purpose of the survey is to assess the potential of hydrothermal submarine ore deposits, in the sea areas of the Kingdom of Tonga, one of the SOPAC member countries. This survey consists of bathymetric survey, sampling, etc., and data analysis.

1-3 The Survey Area

Pursuant to the cooperative study program of Deep Sea Mineral Resources in the economic sea area of SOPAC member countries agreed among the Japan International Cooperation Agency (JICA), the Metal Mining Agency of Japan (MMAJ) and the South Pacific Applied Geoscience Commission, a polygonal area of 36,000 km² formed by joining the following coordinates as shown in Fig.1-3-1 and Fig.2-1-1.

Point No.	Latitude	Longitude
1	19° 20' S	176° 30' W
2	19° 30' S	175° 25' W
3	22° 10' S	175° 50' W
4	22° 00' S	176° 55' W
1	19° 20' S	176° 30' W

1-4 Survey Period

Survey Cruise: from July 2 1995 to September 8 1995 (69 days)

Analysis and Interpretation (Evaluation): from April 1 1995 to March 31 1996

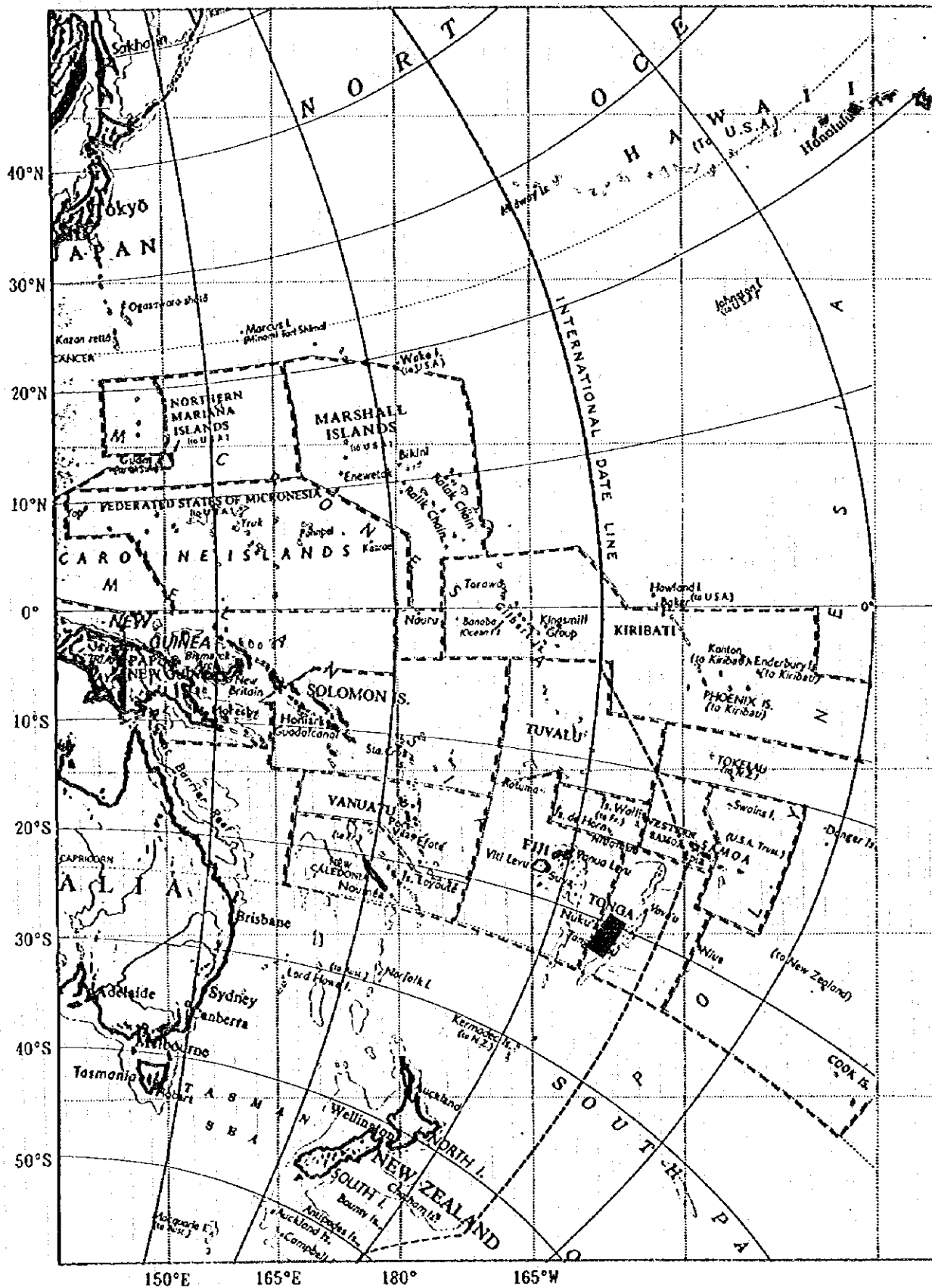


Fig. 1-3-1 Location map of the survey area

1-5 Participants of the Survey

The staff who participated in the survey cruise were delegated by DORD (Deep Ocean Resources Development Co., Ltd.) and OEDC (Ocean Engineering and Development Co., Ltd.).

The members were as follows:

Japanese Participants

Supervisor at Survey sites

Kokichi IIZASA (Geological Survey of Japan) Aug.5-Sep.8

Members

Team Leader & Chief Geophysicist	Kiyoshi KAWASAKI	(DORD)
Chief Geologist	Takumi ONUMA	(DORD)
Geologist	Kazunori MATSUI	(DORD)
Geologist	Nobuyuki OKAMOTO	(DORD)
Geologist	Hironori HISAMATSU	(DORD)
Geologist	Yutaka MATSUURA	(DORD)
Geologist	Hitoshi MORIGAMI	(DORD)
Geologist	Takaya TERAYAMA	(DORD)
Geologist	Kazumi YAMASHITA	(OEDC)
Geophysicist	Nadao SAITO	(DORD)
Geophysicist	Masahiro TAKEDA	(DORD)
Geophysicist	Takao SEO	(DORD)

Geophysicist	Kazuhiko KASHIWASE	(DORD)
Geophysicist	Kazuyoshi FURUYA	(DORD)
Geophysicist	Michiharu ONO	(DORD)
Geophysicist	Keisuke MATSUMURA	(DORD)
Geophysicist	Hisashi SUZUKI	(OEDC)
Geophysicist	Shinichi KUSAKA	(OEDC)
Geophysicist	Shunji HARASHIMA	(OEDC)

Consigning Participants

Adviser

Mr. Andrew W. Goodliffe (University of Hawaii) Jul. 2 - Aug. 8

Trainee

Mr. Tevita Mafoa'acata Fatai (Tonga) Jul. 2 - Aug. 8

Mr. Rennie Jegsen Vaiomo'unga (Tonga) Aug. 6 - Sep. 8

1-6 Apparatus and Equipment for the Survey

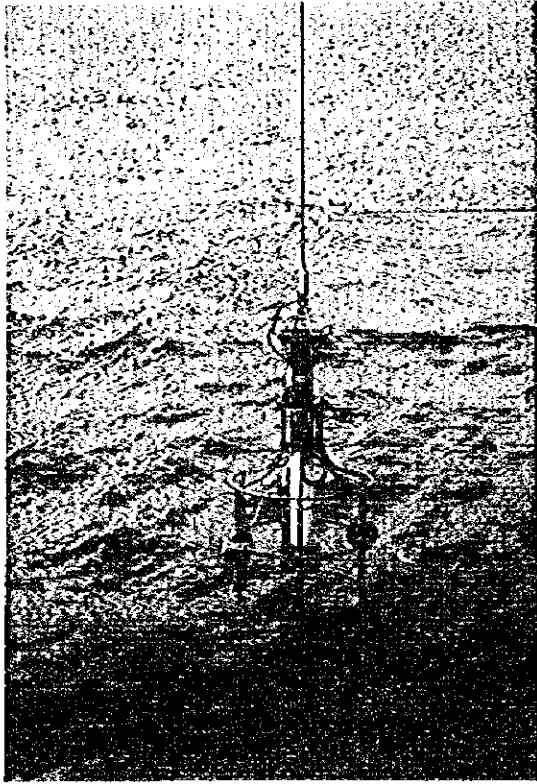
The major apparatus and equipment used during the survey are listed in Table 1-6-1, and shown in Fig. 1-6-1(1)-(3).

1-7 Schedule of the Survey Cruise

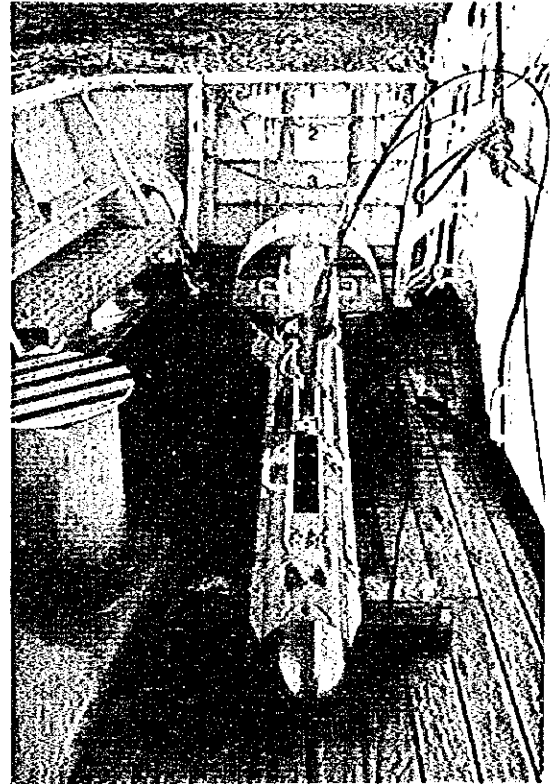
The operation, carried out during the cruise are listed in Table 1-7-1 and the itinerary in Table 1-7-2.

Table 1-6-1 Survey apparatus and equipment

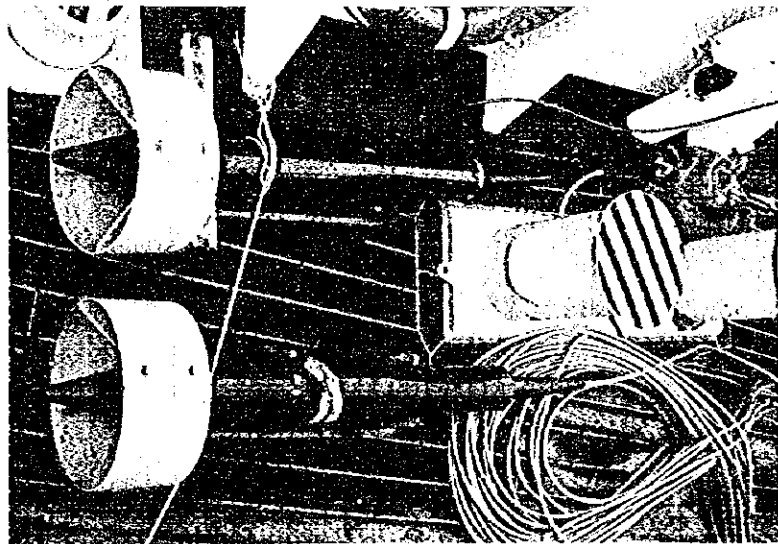
	Survey Method	Survey Apparatus and System	Abbreviation	Remarks
Positioning	Satellite navigation	Global Positioning System	GPS	
Sea Bottom Topography and Geological Survey	Acoustic Sounding Bathymetry	Multi-narrow Beam Echo Sounder	MBES	
		Narrow Beam Echo Sounder	NBS	
	Subsurface Geological Structure	narrow beam Sub-Bottom Profiler	nSBP	
		Side Scan Sonar	SSS	Towed Type
	Magnetic Survey	Proton Radio Meter	PGM	Towed Type
Seawater survey	Conductivity, Temperature and Pressure measuring System	CTD & TD	Vertical Type and Towed Type	
Sea Bottom Observation	Sampling	Large Gravity Corer	LC	
		Chain Bucket	CB	
Sea Bottom Observation	Photograph and TV	Flinder Mounted Power Grab	FPG	
		Continuous Deep Sea Camera With Flinder	FDC	with CTD Towed Type
	Photograph	Deep Sea Camera		with LC
Data Recording and Processing	On-Line Functions Data Storage Functions Off-Line Functions Track Line Maps Various Plan Maps Cross Sections Data Analysis	Data Processing System Sensor CPU File Server CPU Host CPU Engineering Work Station (EWS) Local Areal Network (LAN) Personal Computer (PC) Intelligent Color Monitor (ICM)	DPS	



Conductivity Temperature Depth System (CTD)

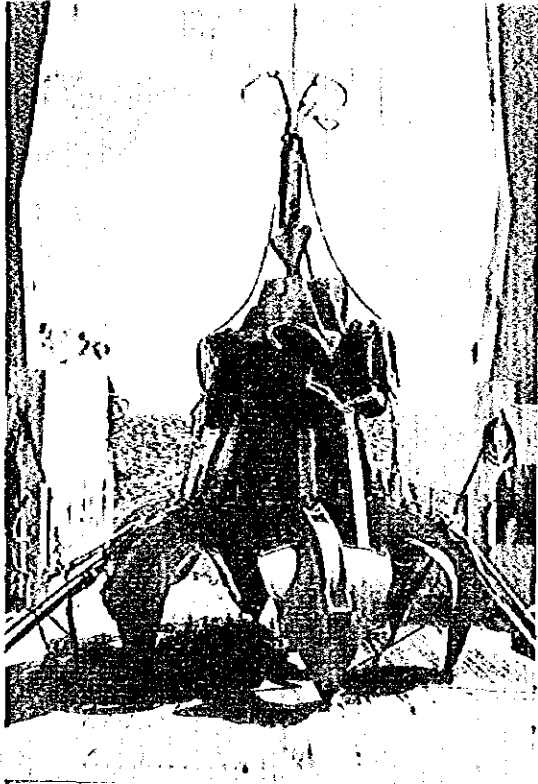


Side Scan Sonar (SSS)

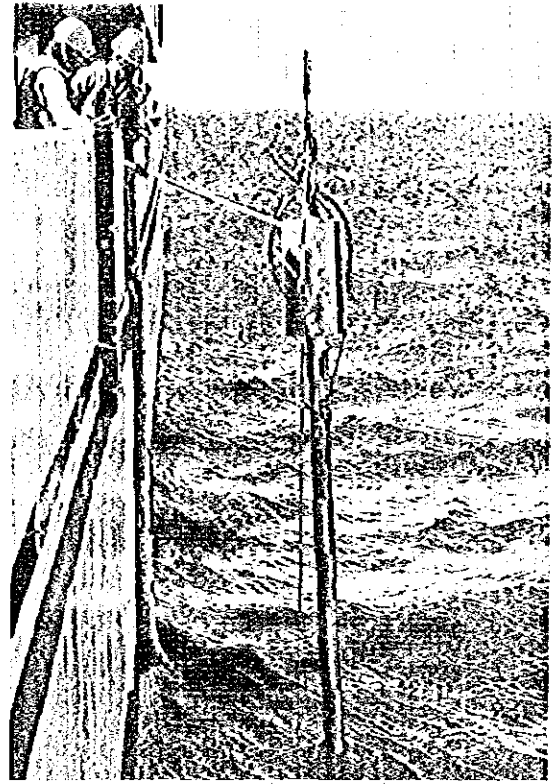


Proton Gradio Meter (PGM)

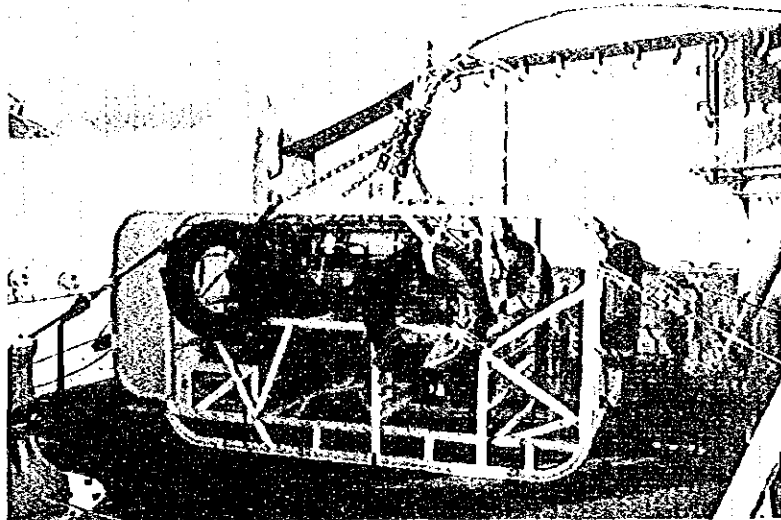
Fig. 1-6-1 (1) Photographs of survey equipments



Finder installed Power Grab (FPG)

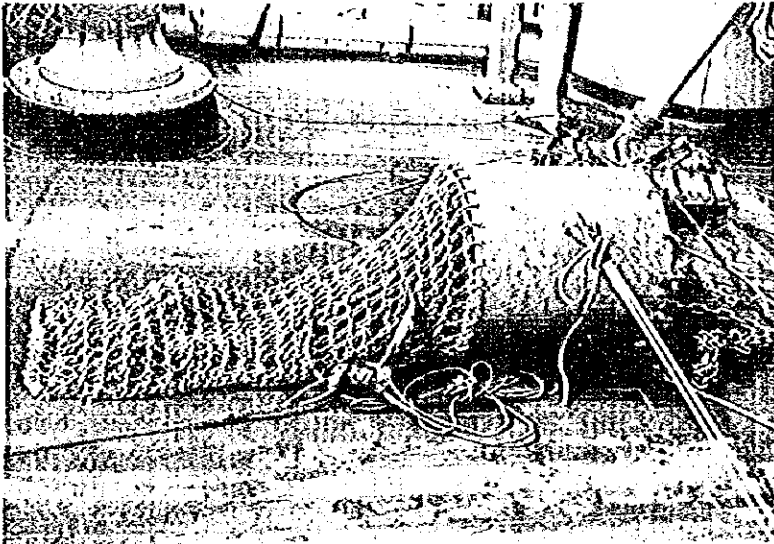


Large Core (LC)

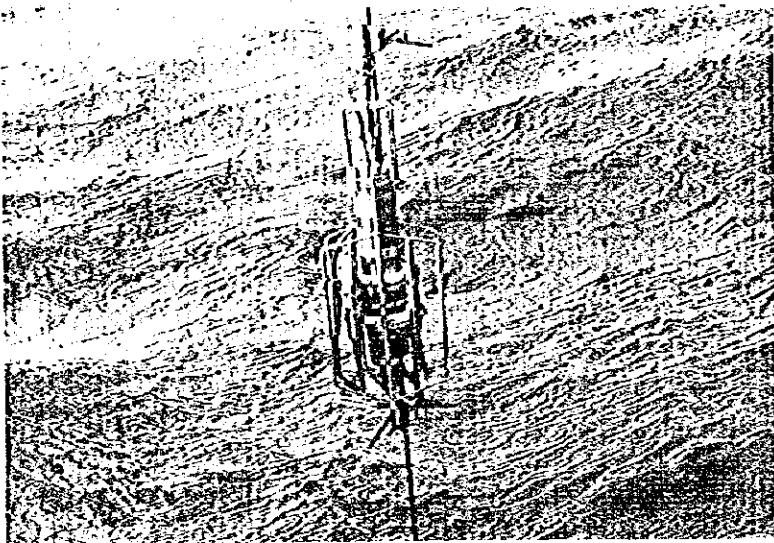


Finder installed Deep-sea Camera (FDC)

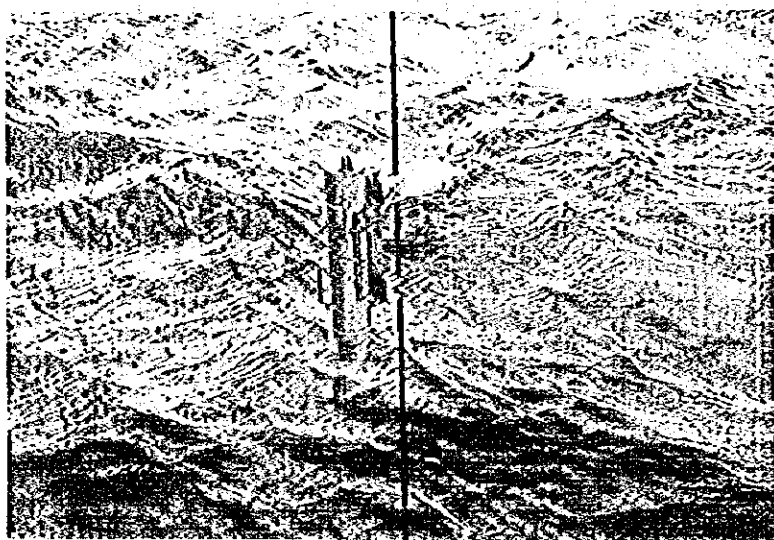
Fig. 1-6-1 (2) Photographs of survey equipments



Chain Bucket Dredge (CB)



Temperature Depth System (TD)



Pinger

Fig. 1-6-1 (3) Photographs of survey equipments

Table 1-7-1 Survey achievements

	Item	Accomplishment	
Survey Schedule	Depart Guam Arrive Survey Area Start the Survey Finish the Survey & Sailing Arrive Nuku'alofa	Jul. 02 16:00 Jul. 13 15:16 Jul. 13 17:10 Aug. 03 16:04 Aug. 04 09:00	Depart Nuku'alofa Arrive Survey Area & Start the Survey Finish the Survey Sailing Arrive Honolulu Aug. 07 16:00 Aug. 08 07:30 Aug. 30 14:10 Aug. 30 16:03 Sep. 08 09:00
Sampling	Weight of Taken Samples	45 points (LC 31 Times, FPG 3 Times, CB 11 Times) Rocks 1,881.8kg Muddy Sediments 405.5kg Total 2,287.3kg	
Deep Sea Observation (FDC)	Number of Track Lines Total Length of the Lines Acquired Photographs	13 Track lines 37.5 nautical miles 1,830 sheets No. 1 line 300 sheets 6.2 miles No. 2 line 126 sheets 2.4 miles No. 3 line 124 sheets 2.4 miles No. 4 line 62 sheets 1.4 miles No. 5 line 94 sheets 1.4 miles No. 6 line 36 sheets 0.7 miles No. 7 line 213 sheets 4.7 miles No. 8 line 148 sheets 3.4 miles No. 9 line 307 sheets 6.3 miles No. 10 line 135 sheets 3.3 miles No. 11 line 53 sheets 1.3 miles No. 12 line 77 sheets 1.8 miles No. 13 line 155 sheets 2.1 miles	
Physical Property Survey	CTD (Vertical Type) (Towed Type)	27 Points 25 lines (with FDC, FPG, CB)	
Acoustic Sounding	MBES (15.5kHz) NBS (30.0kHz) nSBP (3.5kHz) SSS (59.5kHz)	6,060.6 miles 6,060.6 miles 6,060.6 miles 49.7 miles (3 lines)	
Magnetic Survey (PCM)	Proton Magnetometer	4,891.0 miles	
Data Processing	MT from Data Processing System (No. 5 Labo) MT from MBES Drawing	1 reel (Off-Line) 31 reel (On-Line) Track Line Map, Bathymetrical Maps, Cross Sections etc.	

Date and Time are shown in the Local Time.

Table 1-7-2 Records of survey schedule

Survey Items (Leg 1)		Survey Items (Leg 2)	
Month/Day	Survey Items (Leg 1)	Month/Day	Survey Items (Leg 2)
01			
02			
03			
04			
05			
06			
07			
08			
09			
10			
11			
12	01 07/02 Su 16:00 Departure from Guam	08/07 Mo	Departure from Nuku'alofa
13	02 07/03 Mo Sailing (3, 09nm from Guam to the survey area)	08/08 Tu	Moving to the survey area
14	03 07/04 Tu --ditto--	08/09 We	FDC survey (No. 11line) & Bath. survey
15	04 07/05 We --ditto--	08/10 Th	SSS survey (No. 11line) & Bath. survey
16	05 07/06 Th --ditto--	08/11 Fr	SSS survey (No. 21line) & Bath. survey
17	06 07/07 Fr --ditto--	08/12 Sa	SSS survey (No. 31line) & Bath. survey
18	07 07/08 Sa --ditto--	08/13 Su	FDC survey (No. 2, No. 31line) & Bath. survey
19	08 07/09 Su --ditto--	08/14 Mo	FDC survey (No. 4, No. 51line) & Bath. survey
20	09 07/10 Mo --ditto--	08/15 Tu	FDC survey (No. 6, No. 71line) & Bath. survey with PGM
21	10 07/11 Tu --ditto--	08/16 We	FDC survey (No. 81line) & Bath. survey with PGM
22	11 07/12 We --ditto--	08/17 Th	Bathymetric survey & Bath. survey with PGM
23	12 01 07/13 Th 15:46 Arrival in the survey area. CTD survey	08/18 Fr	FDC survey (No. 91line) & Bath. survey with PGM
24	02 07/14 Fr Bathymetric survey with PGM	08/19 Sa	FDC survey (No. 10, No. 111line)
25	03 07/15 Sa Bathymetric survey with PGM	08/20 Su	FDC survey (No. 12, No. 131line)
26	04 07/16 Su Bathymetric survey with PGM	08/21 Mo	Ore sampling (3) & Bath. survey
27	05 07/17 Mo Bathymetric survey with PGM	08/22 Tu	Ore sampling (3) & Bath. survey
28	06 07/18 Tu Bathymetric survey with PGM	08/23 We	Ore sampling (4) & Bath. survey
29	07 07/19 We Bathymetric survey with PGM	08/24 Th	Ore sampling (4) & Bath. survey
30	08 07/20 Th Bathymetric survey with PGM	08/25 Fr	Ore sampling (3) & Bath. survey
31	09 07/21 Fr Bathymetric survey with PGM	08/26 Sa	Ore sampling (2) & Bath. survey
32	10 07/22 Sa Bathymetric survey with PGM	08/27 Su	Ore sampling (4) & Bath. survey
33	11 07/23 Su CTD, Bathymetric survey with PGM	08/28 Mo	Sampling (3) & Bath. survey
34	12 07/24 Mo Bathymetric survey with PGM	08/29 Tu	Sampling (3) & Bath. survey
35	13 07/25 Tu Bathymetric survey with PGM	08/30 We	Sampling or Baseline Geochemical survey & Departure from the survey area
36	14 07/26 We Bathymetric survey with PGM	08/31 Th	--ditto--
37	15 07/27 Th Bathymetric survey with PGM	09/01 Fr	--ditto--
38	16 07/28 Fr Baseline geochemical sampling (4)	09/02 Sa	--ditto--
39	17 07/29 Sa Baseline geochemical sampling (5)	09/03 Su	--ditto--
40	18 07/30 Su Baseline geochemical sampling (5)	09/04 Mo	--ditto--
41	19 07/31 Mo Bathymetric survey with PGM	09/05 Tu	--ditto--
42	20 08/01 Tu Bathymetric survey with PGM	09/06 We	--ditto--
43	21 08/02 We Bathymetric survey with PGM	09/07 Th	--ditto--
44	22 08/03 Th Departure from the survey area	09/08 Fr	09:00 Arrival in Honolulu
45	23 08/04 Fr 09:00 Arrival in Nuku'alofa		
46	24 08/05 Sa in Nuku'alofa		
47	25 08/06 Su in Nuku'alofa		
48			
49			
50			
51			
52			
53			
54			
55			
56			
57			
58			
59			
60			
61			
62			
63			
64			
65			
66			
67			
68			
69			

Date and Time are shown in Local Time.

CHAPTER 2 SURVEY METHOD

2--1 Survey Plan

In 1995, the first fiscal year of the third phase of the five-year SOPAC program, a survey on submarine hydrothermal ore deposits and bathymetric survey was carried out, as planned, within the exclusive economic zone of the Kingdom of Tonga as shown in Fig.2-1-1.

A regional survey was carried out in the survey area during the first half of the schedule (LEG 1). The regional survey was composed of topographical and magnetic surveys at intervals of 2 miles and baseline geochemical samplings. During the second half of the schedule (LEG 2), areas for carrying out the ore deposit investigation were selected on the basis of the results obtained from the bathymetric and magnetic surveys. Deep-sea observation by FDC, SSS surveys and sampling were carried out in the selected areas.

Principal works for the survey were comprised of the following;

1. Bathymetric surveys were carried out at 10 knots by using GPS and MBES to identify geographical features accurately. The bathymetric survey at a supplementary line interval of one nautical mile was adopted in shallow sea area.
2. Magnetic surveys were also carried out simultaneously with the Bathymetric surveys to estimate the geological structure.
3. Samples for the baseline geochemical survey were collected in an area with a coordinate of $21^{\circ} 05' S$ and $176^{\circ} 15' W$ as its center (14 sampling points).
4. SSS survey was carried out on three lines with a total line length of 49.7 nautical miles in the selected sea area by bathymetric map and acoustic reflection image to identify the precise topography and distribution of bottom sediments.
5. Continuous deep sea observation by FDC was carried out at 13 track lines with a total line length of 37.5 nautical miles.
6. Sampling of rocks and sediments were made by FPG at three points, LC at 17 points (total 31 points including geochemical sampling) and CB at 11 points.

2--2 Numbering

Survey lines and sampling points were numbered in the following ways;

Sampling points for the survey on ore deposits:

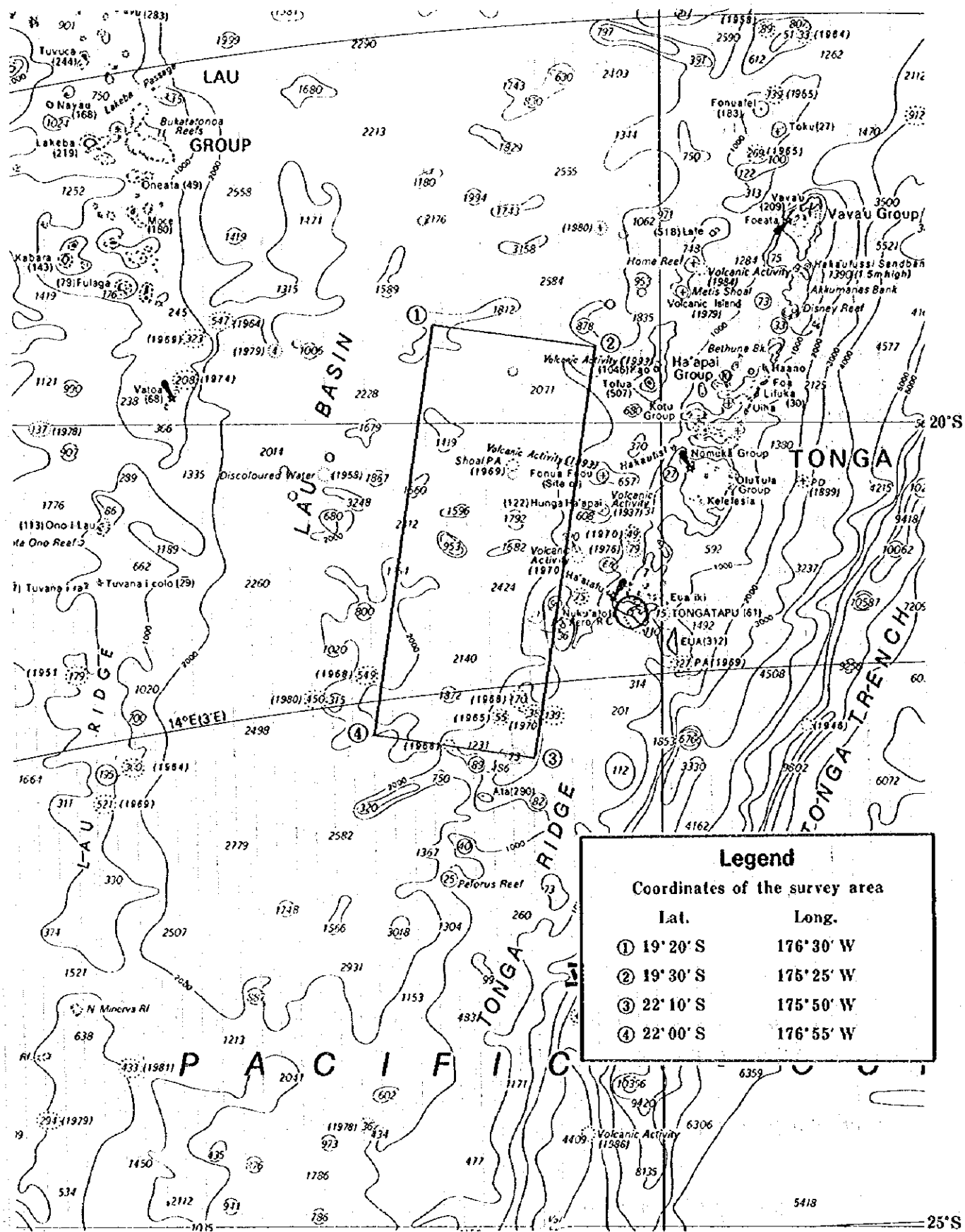


Fig. 2-1-1 Survey planning map

Year - S - Equipment used - No.

Example : 95SFPG01 (in the case where FPG was employed)

95SLC01 (in the case where LC was employed)

95SCB01 (in the case where CB was employed)

In this case, "S" represents SOPAC and "No." indicates the serial number.

The sample number in the chapter 5 consists of the sampling points number (above example) and the identification letter (below example) after that.

C:Chemical analysis (major components)

M:Chemical analysis (base metal elements)

N:Chemical analysis (rare earth elements)

R:C+M+N

T:Thin section observation

P:Polish observation

X:X-ray diffraction analysis

K:Age determination (K-Ar method)

F:Micro fossil observation

SSS survey lines:

Year - S - SSS - No.

Example : 95SSSS01

In this case, "S" represents "SOPAC" and "No." indicates the serial number.

FDC survey lines:

Year - S - FDC - No.

Example : 95SFDC01

In this case, "S" represents "SOPAC" and "No." indicates the serial number.

Acoustic sounding survey lines:

No. - division - 0 to 9

Example : 16 - 0 - 0

In this case, "No." indicates line number of the main line with serial number from North at two nautical miles interval, and "division" indicates the number of divided line with serial number from 0. The last number 0 to 9 indicates the supplementary line number.

2-3 Ship Positioning and Positions of Towed Fish

The position of the ship was measured by GPS. The position of the towed vehicle was calculated from the depth measured by a CTD Sensor, which was mounted on the towed vehicle and the length of the cable by applying the Pythagorean formula.

As for the system of geodetic coordinates, WGS84 was used, and the 175° W Local Time (GMT +13 hours) was used for the onboard time.

2-4 Acoustic Sounding

Bathymetric survey was carried out at an interval of two nautical miles covering the entire survey area, and especially in the shallow area, supplemental lines were adopted in between the main lines. Extremely shallow areas less than 500 m were eliminated from the survey area (Fig.2-4-1).

The bathymetry readings were made at every 5 to 10 seconds from MBES and every 8 second for NBS while the vessel was cruising at 10 knots.

2-5 Magnetic Survey

Magnetic survey was carried out simultaneously with bathymetric survey as a help toward the geological structure interpretation. The magnetic data were collected on the main lines for bathymetric survey.

In order to protect the magnetic sensor from magnetism of the vessel, the magnetic sensor was towed from the stern by a cable and the distance from the stern to the sensor was maintained at 710 m. Total magnetic force was measured by the sensor at the sensitivity of 0.1 gamma every 6 second. Measured data were on-line recorded in the DPS every 10 second before the data were processed.

2-6 Seafloor Observation and Photographing

Real time seafloor observation was made through color TV image by towing the FDC, on which a still camera, a TV camera and a CTD sensor were loaded at the cruising speed of 1 knot, and color photographs were taken at characteristic points. Seafloor images were recorded onto videotapes. The lengths of the track lines were set about 0.7 - 6.3 nautical miles. The towing direction was selected properly by considering the direction of tide and wind. (Fig.4-1-2).

2-7 Sampling

The baseline geochemical sampling was made at 14 points along the line of about 10 nautical miles, which were set approximately oblique to the ridge with its center near the coordinates of 21° 05' S and 176° 45' W (Fig.4-1-2(3)), 95SLC01 to 95SLC14. Sampling was carried out about four times a day on

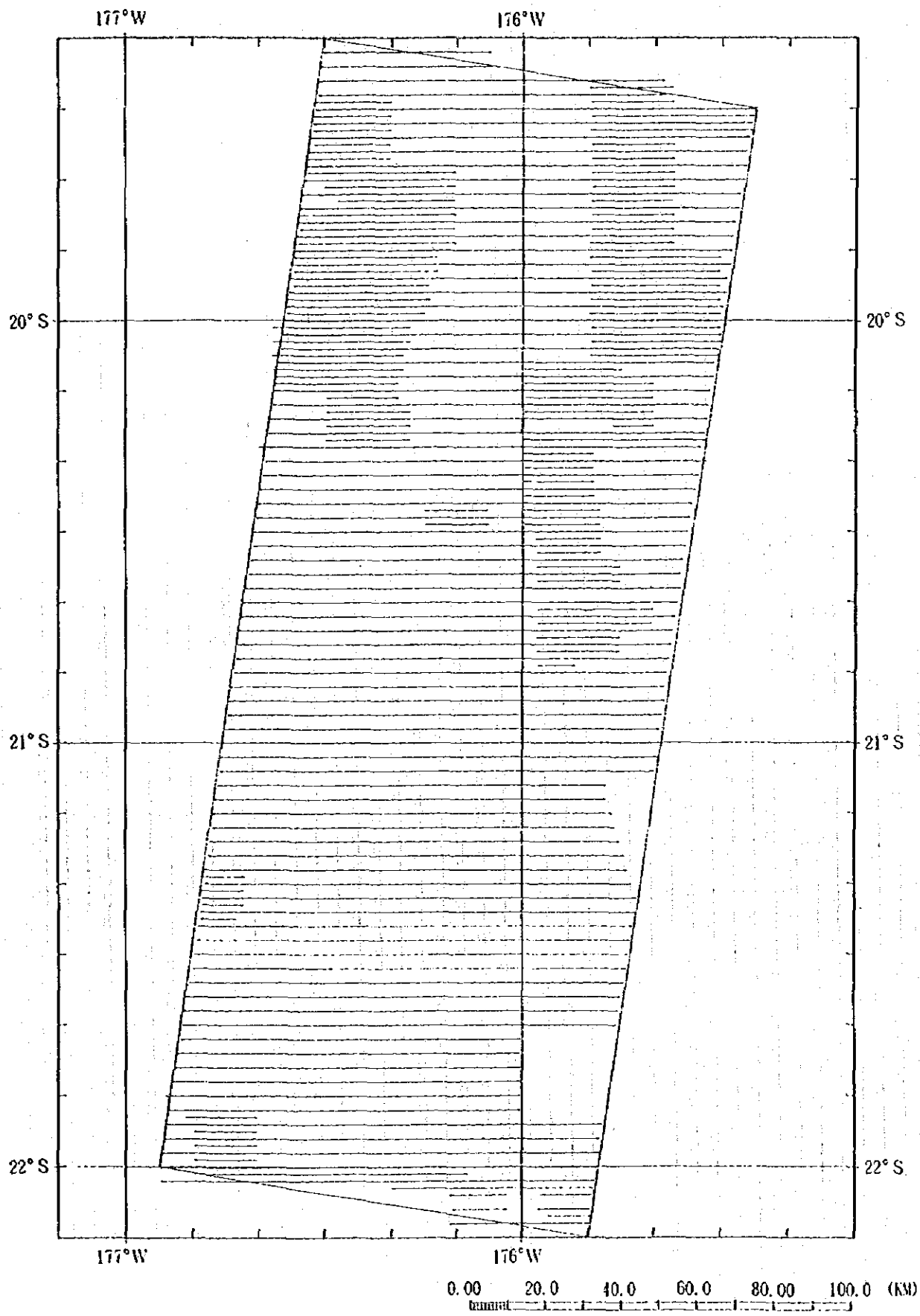


Fig. 2-4-1. Location map of track line

average by LC.

Other sampling points were decided in reference to the results of bathymetric survey, acoustic reflection image and the results of SSS and FDC surveys which were done before.

2--8 Sea Water Survey (CTD Measurement)

A vertical CTD survey was carried out at two points as the MBES requires values of sound velocity versus depth.

Also, to detect the signs of hydrothermal activity, data on water temperature, salinity and water pressure were collected every 5 second by the CTD mounted on FDC, for analysis.

Furthermore, depth data which was calculated from the CTD data was used to calculate the location of the towed fish.

2--9 Data Processing and Analysis

Data processing and analysis were made by DPS and personal computers as shown in the Data Processing and Analysis Flowsheet (Fig.2-9-1). Fundamental data processing and analysis were done on board, and a cruising report was prepared.

Afterwards, various tests, studies and analyses were made on shore and the present report was produced by combining them.

Chemical analysis, X-ray diffraction analysis, dating and microscopic observation were done on rock samples.

Chemical analysis and microfossil observation were done on sea floor sediments.

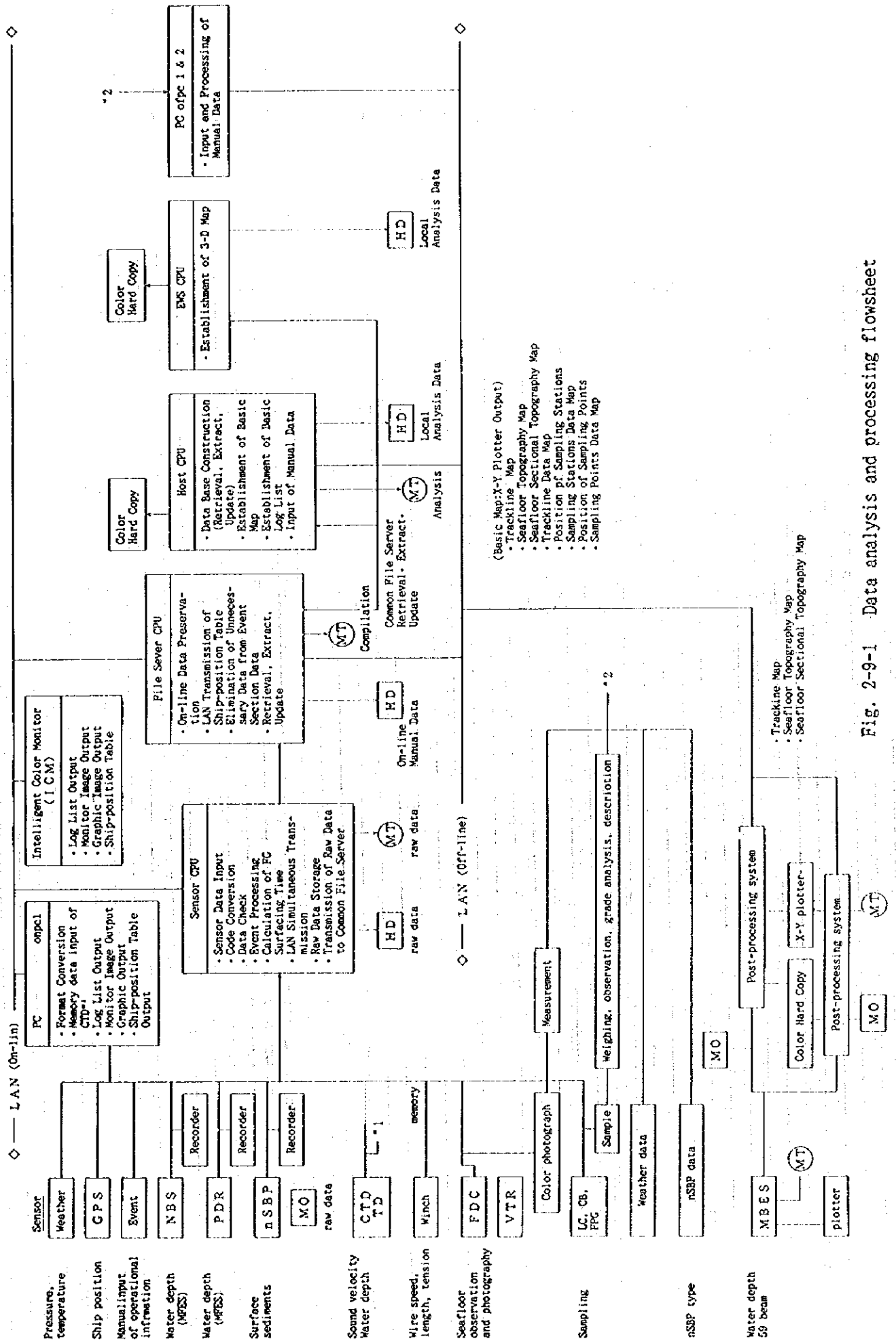


Fig. 2-9-1 Data analysis and processing flowsheet

CHAPTER 3 BATHYMETRY AND GEOLOGICAL STRUCTURE

3-1 Tectonic Setting around the Survey Area

The survey area locates in the middle to eastern part of Lau Basin in the west of the Tonga Islands, which array in NNE-SSW direction in about 3,000 km east of Australia, lying from 15° S to 24° S in latitude. In the east of Tonga Islands, the Tonga Trench exists in parallel to the islands with a maximum depth of over 10,000 m, where the Pacific Plate subducts under the Australian Plate towards west. The Lau Basin is a back-arc basin behind the Tonga Trench. The eastern margin of the Lau Basin corresponds to the Tonga Ridge (the Tonga Islands) and the western margin to the Lau Ridge. These structure are listed from east to west as follows (See below figure);

Tonga Trench: Subduction zone of the Pacific Plate.

Tonga Ridge (Tonga Islands): Island arc, volcanic arc.

Tofua Volcanic Arc: Current volcanic front where active volcanic activities are taking place.

Lau Basin: Spreading back-arc basin.

Hydrothermal ore deposits and activities are occurring.

Lau Ridge: Old island arc.

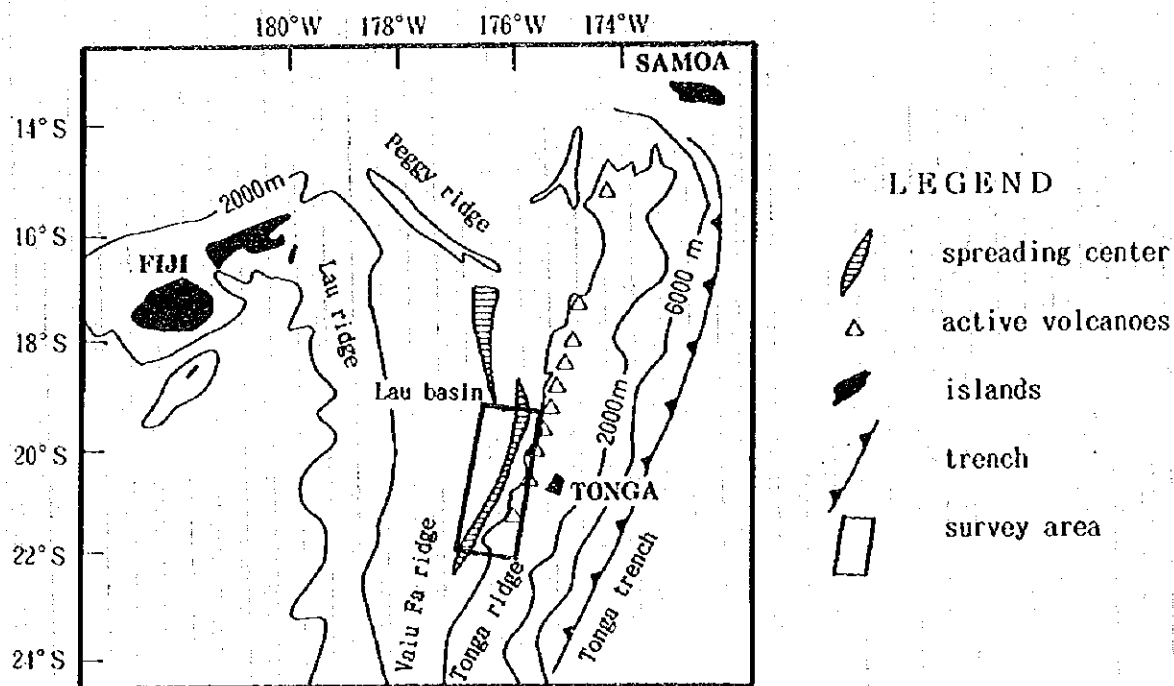


Fig. 3-1-1 Tectonic setting map around the survey area

The Lau Basin forms a reverse triangle shape elongated in north-south direction between Tonga Ridge stretching in NNE-SSW direction and Lau Ridge in north-south trending. There are two spreading axes in NNE-SSW direction in the central part of northern basin and the eastern part of southern basin. The southern spreading center is called the Valu Fa Ridge.

The survey area in north-south elongated shape includes most of the Valu Fa Ridge as its center.

The spreading axis in the Lau Basin started to open from north, propagating towards east and south. The northern spreading axis began spreading 5-3 Ma, then MORB type tholeiitic basalt erupted in the spreading center and island-arc type volcanic activities began to occur in the Lau Ridge. The southern spreading axis was newly formed 3-1 Ma, where more classified island-arc type volcanic rocks erupted and there are various types of volcanic rocks mainly as basalt to dacite. The southern spreading center is propagating towards south even now.

Several hydrothermal ore deposits have been discovered near the spreading center in the Lau Basin. Especially in the southern part of the Valu Fa Ridge, an active hydrothermal ore zone was confirmed. Various hydrothermal phenomena such as chimneys of sulfides and barite, massive sulfides, and vein to network sulfides were observed here. The hydrothermal ore deposits found in the southern part of the Lau back-arc basin (Valu Fa Ridge) has the intermediate characters of two types; young back-arc basin type (for example, the Okinawa Trough) and matured back-arc type (near midocean ridge type, for example, North Fiji Basin) (Y.Fouquet et al., 1993).

The survey area includes the northern part of hydrothermal activity zone in the south of the Valu Fa Ridge.

3-2 Bathymetry

The survey area locates in the middle eastern part of the Lau Basin, west of the Tonga Islands. There is a spreading center in the direction of NNE-SSW as the northern extended zone of the Valu Fa Ridge. A color-coded bathymetric map obtained by the bathymetric survey and typical bathymetric profiles are shown in Fig. 3-2-1, 3-2-2, and 3-2-3, respectively, and all the bathymetric profiles are shown in Appendix Fig. 1.

The main characteristics of the seafloor topography can be summarized as follows;

- (1) Water depth in the northern part of the survey area is rather deep with a maximum depth of 3,250 m, and it gradually becomes shallower towards south.
- (2) Seafloor topography apparently varies in the eastern and the western side of the spreading center as its center; Topography of the western cliff is complex and rugged (a maximum height difference is around 500 m), while the eastern cliff is rather gentle (a maximum height difference is around 200

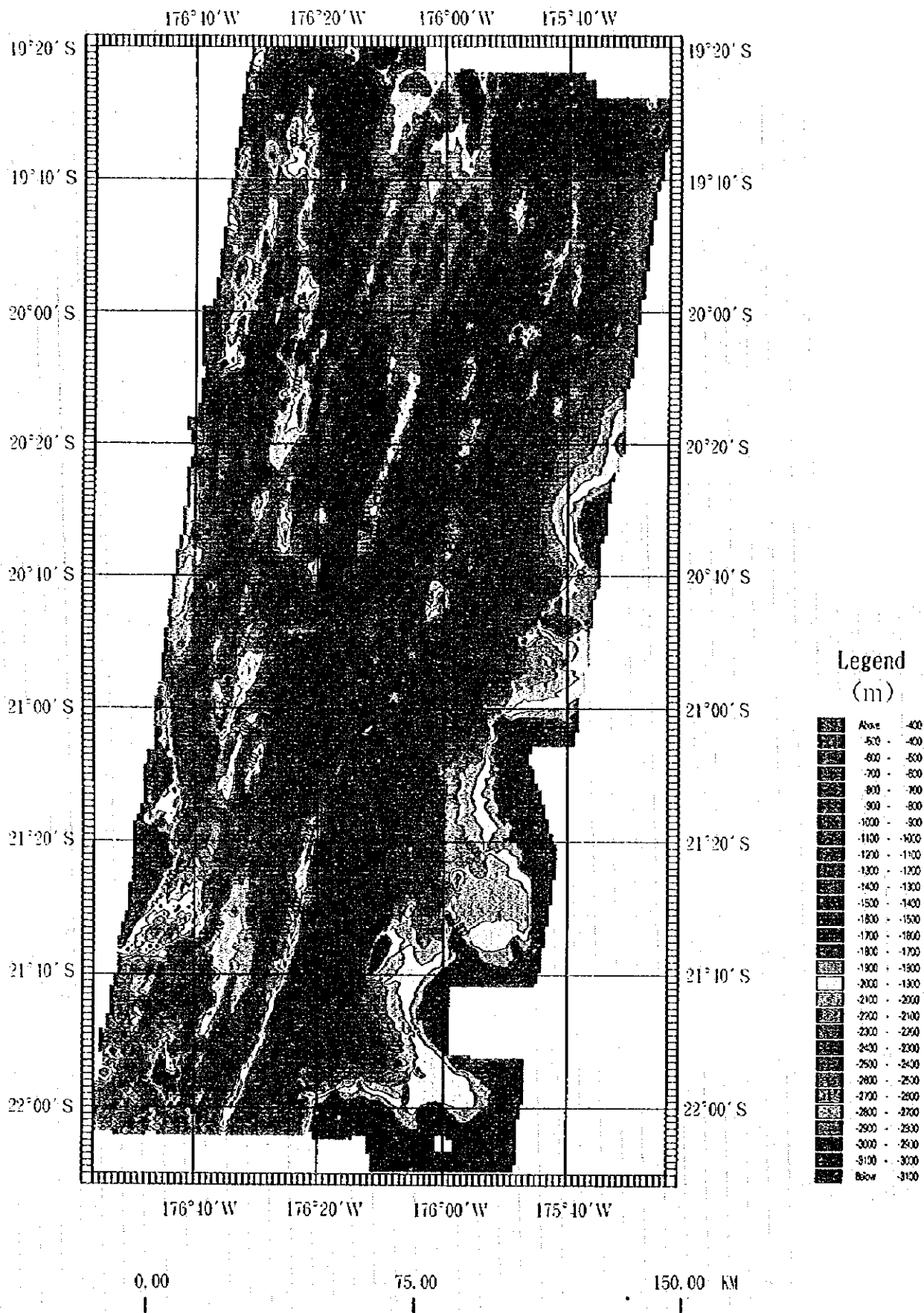
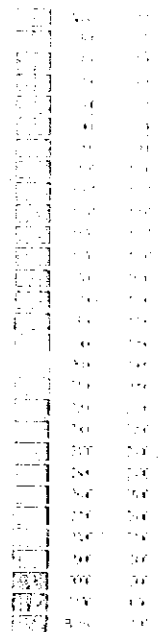
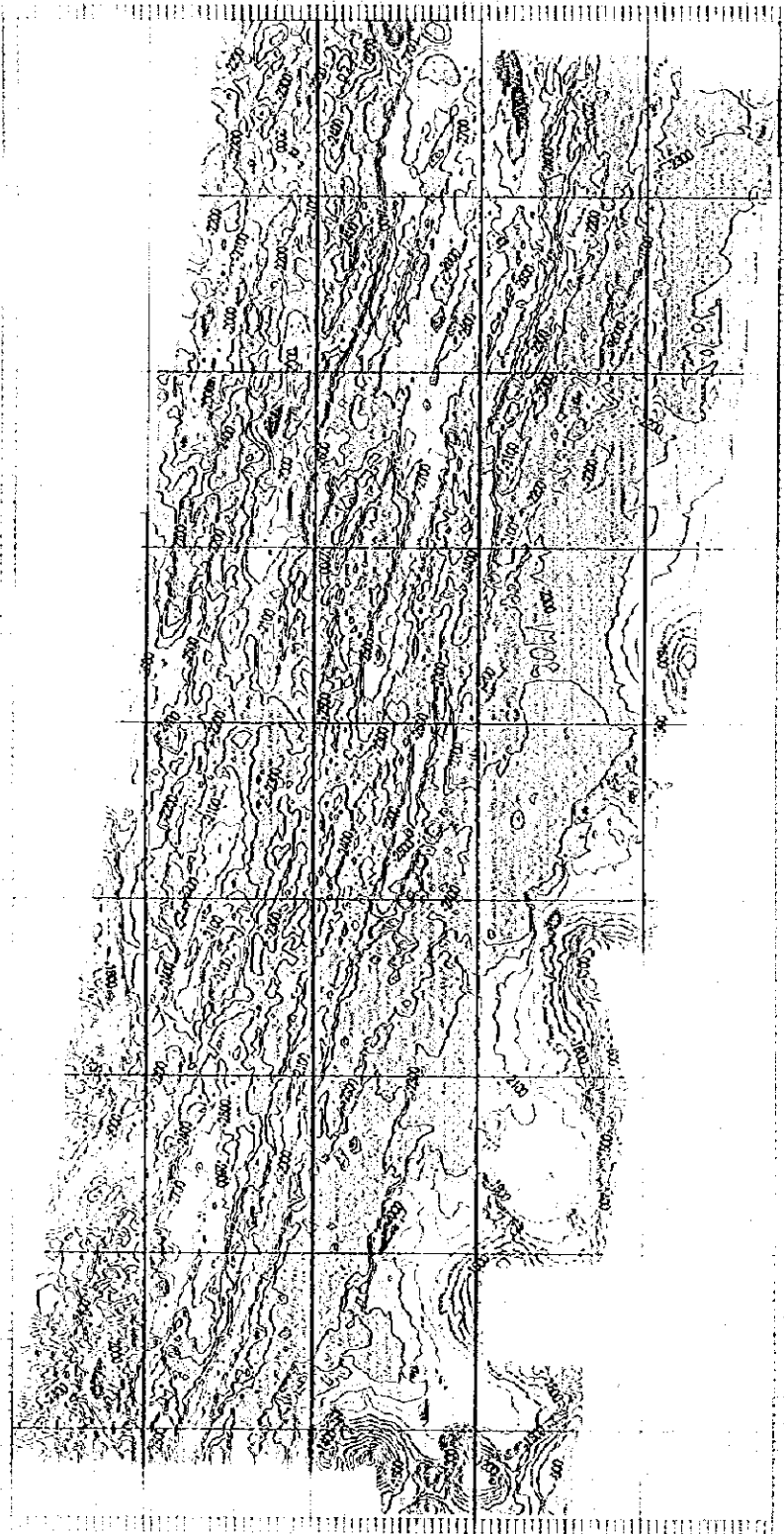


Fig. 3-2-1 Color-coded bathymetric map based on MBES.
Color change and contour interval is every 100m



This map was prepared by the U.S. Geological Survey, Reston, Virginia, and is available in digital form on the National Geospatial Data Archive (NGDA) website at <http://www.ngda.gov>. For more information, contact the National Geospatial Data Archive at ngda@usgs.gov.

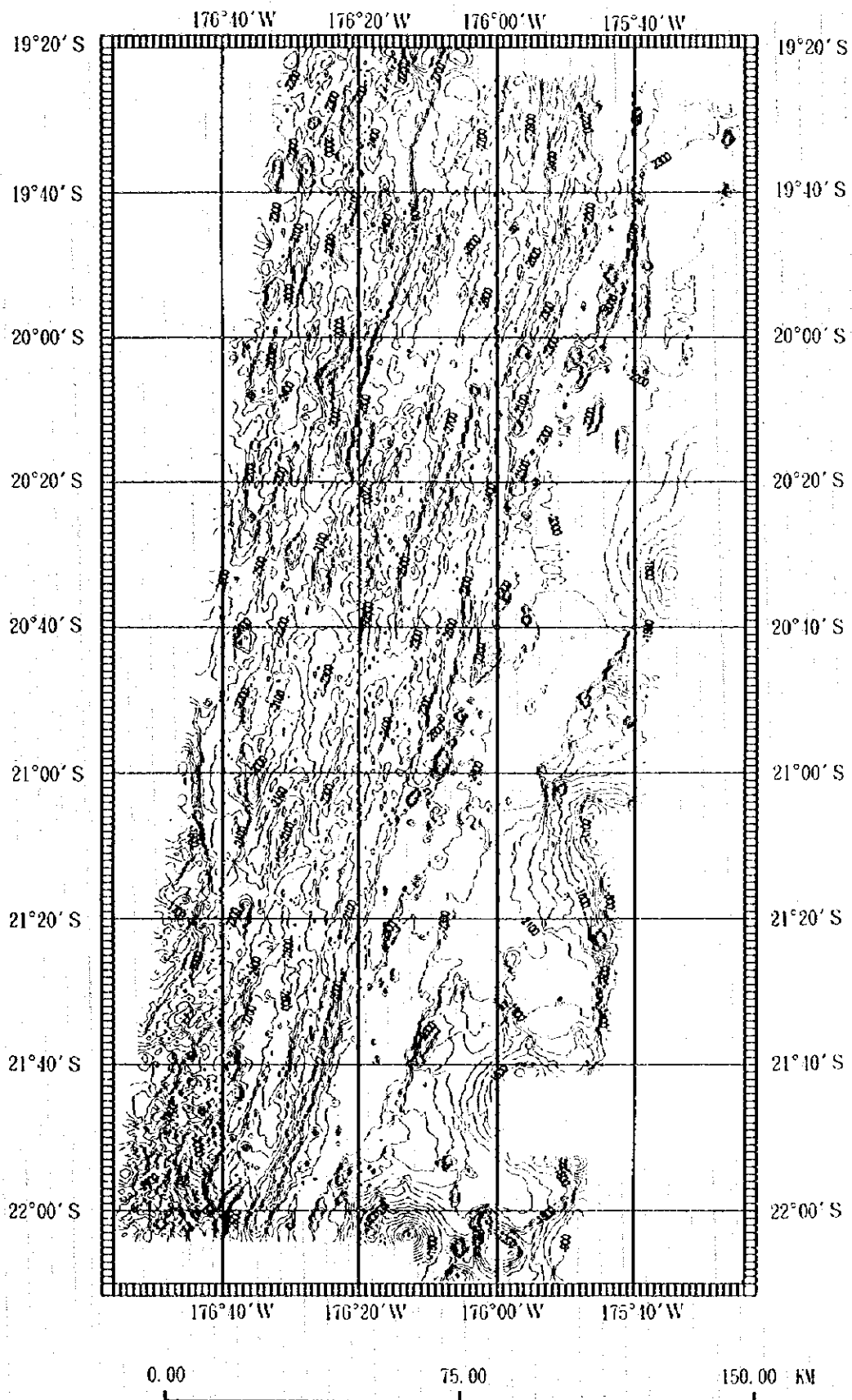


Fig. 3-2-2 Bathymetric map based on MBES.
 MBES data are gridded at an about 1.5km spacing
 Contour interval is 100m.

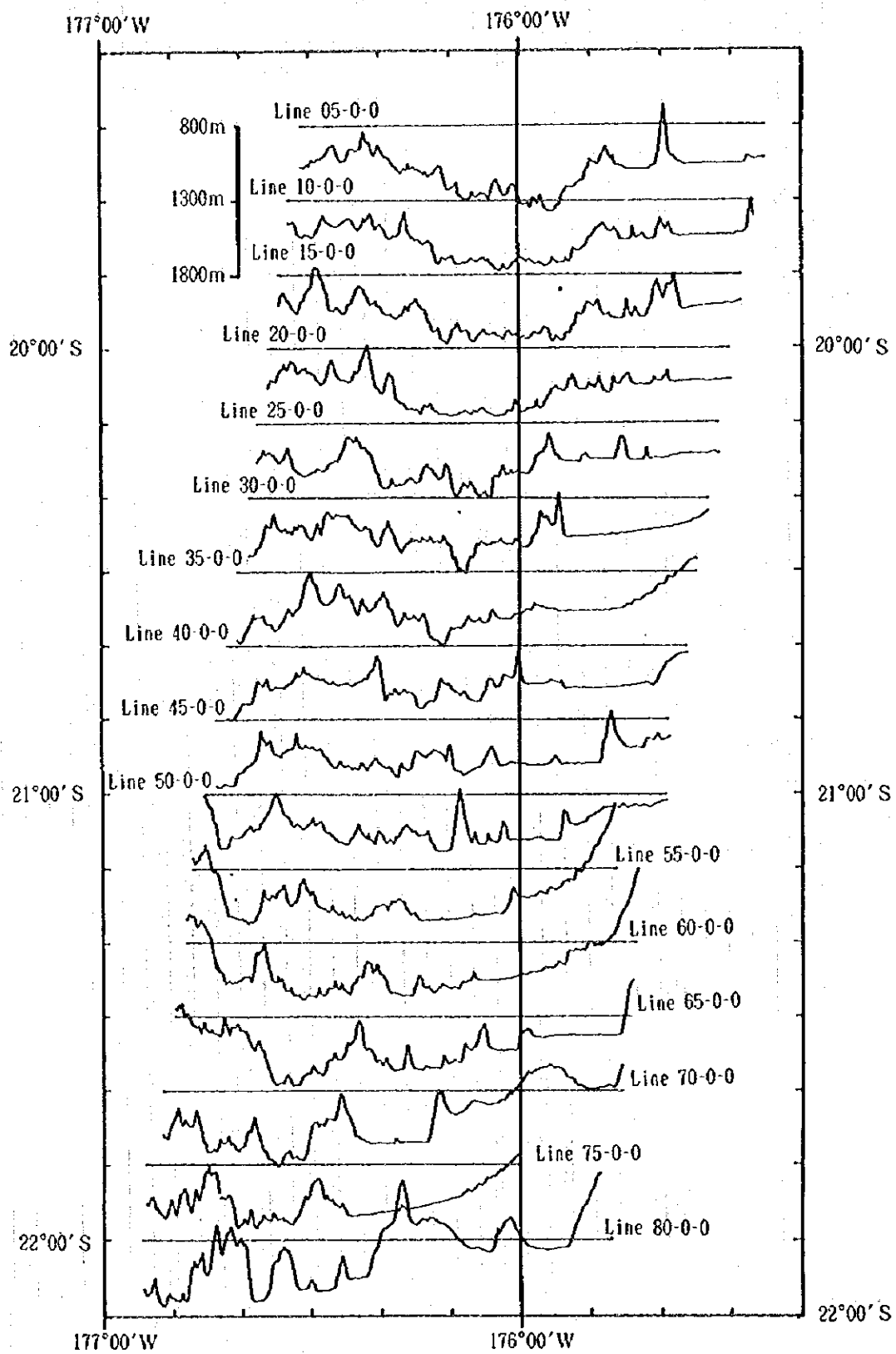


Fig. 3-2-3 Bathymetric profiles

m).

(3) There are numerous seamounts and knolls in close and in parallel with the spreading center.

- Seamounts and knolls in the west of the spreading center;

There are seamounts and knolls at shallower depth than 2,200 m, extending in north-south direction. They are bigger in scale than the eastern side. In the western side of the spreading center, there is also a knoll with caldera near $20^{\circ} 12'S, 176^{\circ} 25'W$. The length of axes of this knoll is about 4 km and the height difference is about 200 m. The size of the caldera is 2 km in a longer axis and 1.5 km in a shorter axis.

- Seamounts and knolls in the east of the spreading center;

The scale of the seamounts and knolls in the east is smaller than those in the west. The seamounts and knolls in the north of $20^{\circ} 50'S$ are studded in north-south direction like as the ones in the western side of the spreading center. In the south of $20^{\circ} 50' S$, some knolls are seen at a water depth of about 2,500 m.

(4) In the vicinity of $21^{\circ} 40'S, 176^{\circ} 36'W$ in the southwestern part of the area, there is a trough with a long axis of about 55 km and a short axis of about 20 km. The deepest part is about 2,800 m.

(5) The spreading center shows graben in the north, and from the center ($20^{\circ} 40'S$) towards south, it becomes a ridge shape. Many ridges are seen in the southern area.

(6) The spreading center shows an overlapping spreading center with a trough in between them in the area between $20^{\circ} 00'S$ to $20^{\circ} 40'S$. This trough is an axial graben with a longer axis of about 65 km and a shorter axis of 6 km, and its deepest part is about 2,800 m. The eastern slope of this axial graben shows terrace shape, which lies in a water depth shallower than 2,600 m, and the width is about 200 m and the length is about 2 km.

(7) As a knoll found in the vicinity of $19^{\circ} 55'S, 176^{\circ} 04'W$ in the north, several topographic features are seen suggesting a split to east and west with the spreading center as its center.

3-3 Magnetic Survey

(1) Total Magnetic Force

The magnetic survey was carried out simultaneously with bathymetric survey with a survey line spacing of 2 nm in the survey area. Data acquisition of total magnetic force was made twice in the area where data quality was poor or data were partly lacking. No magnetic storm was observed and during the whole survey period no diurnal magnetic corrections were made. After data acquisition, a total magnetic force map as shown in Fig. 3-3-1 was made with each grid point at 1,500 m interval by interpolating the observed values. Contour interval is 100 nT in each map.

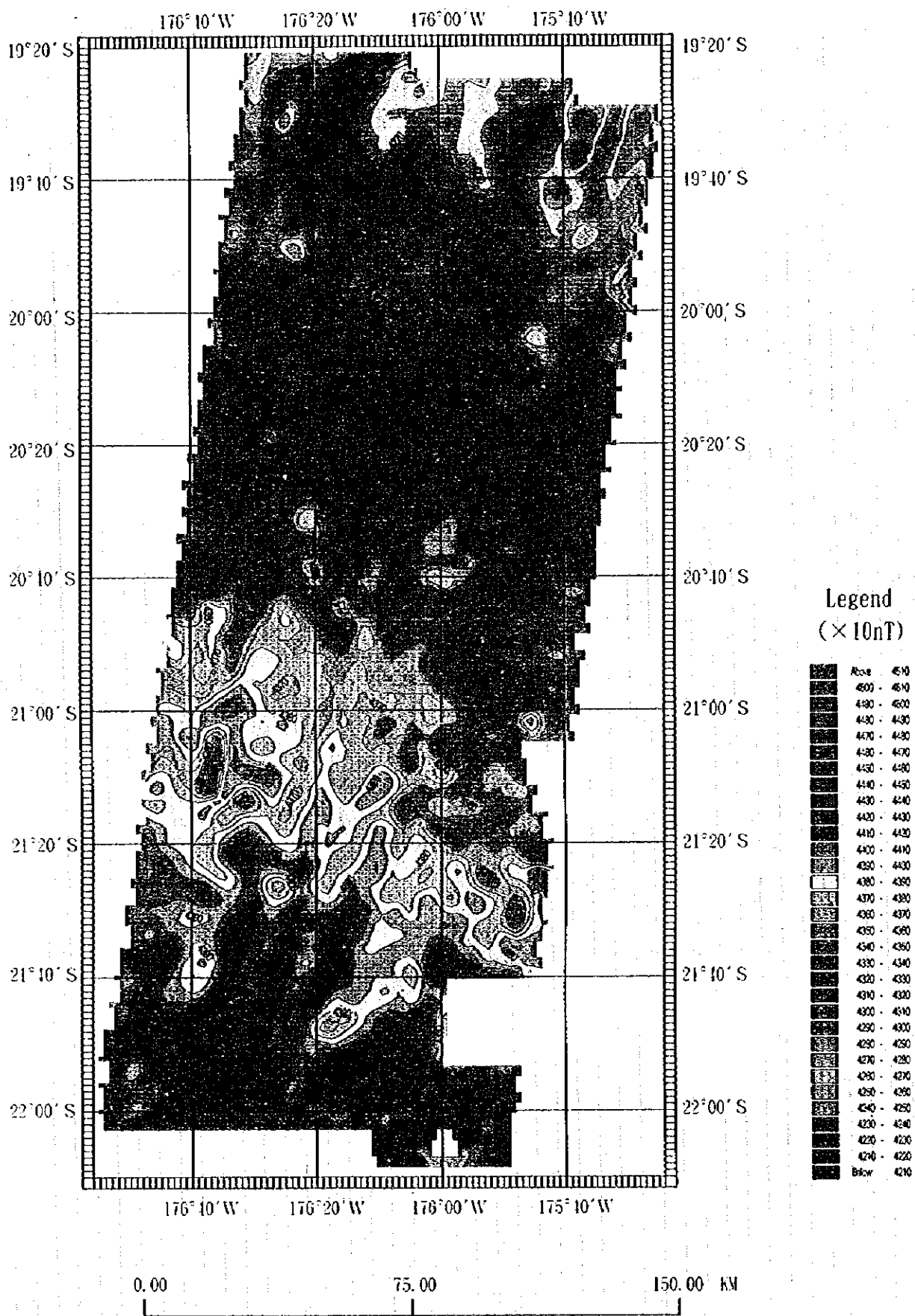
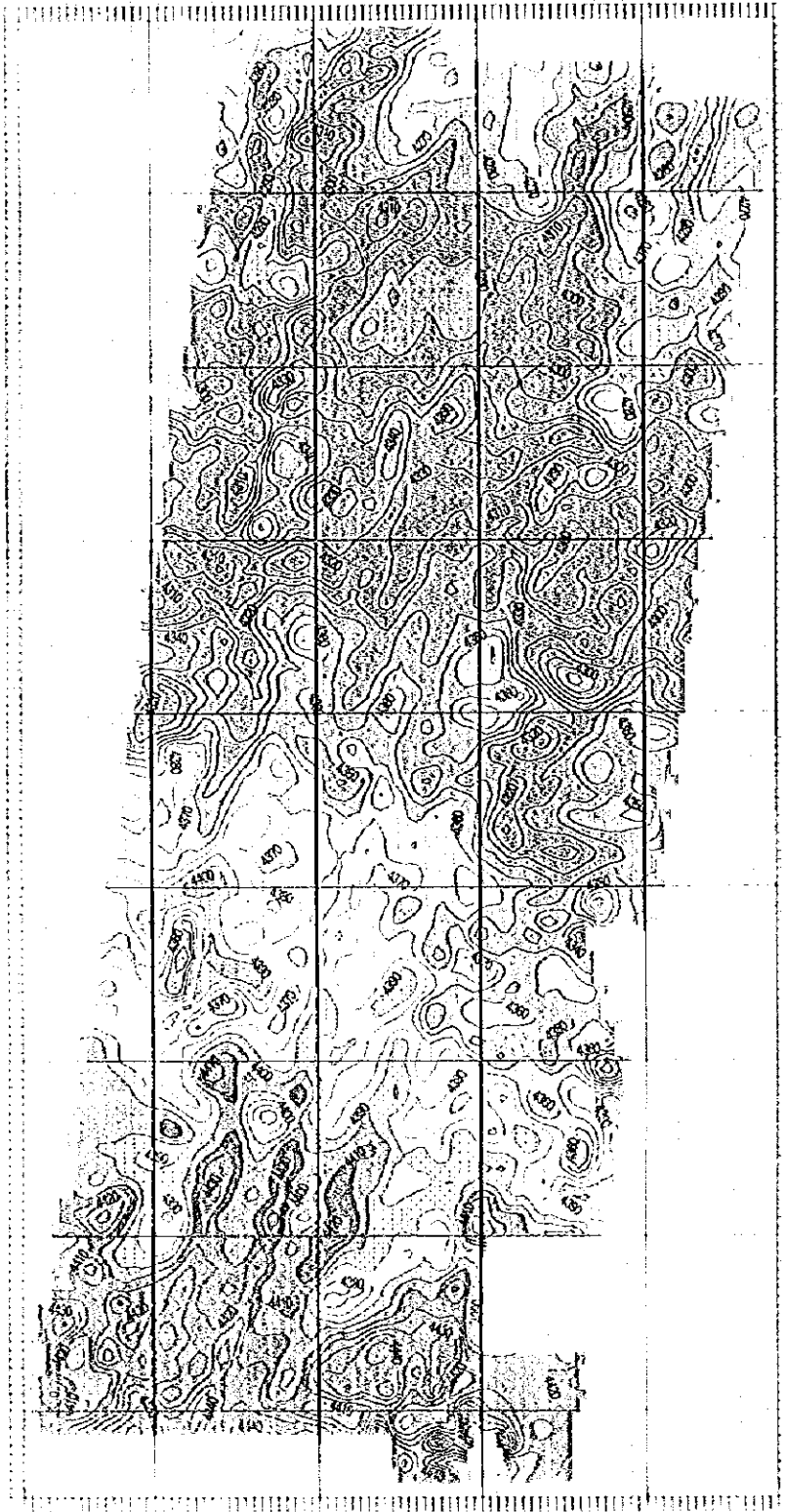


Fig. 3-3-1 Total magnetic force map gridded with a spacing of 1.5km. Isomagnetic lines are at 100nT intervals.



100	100
200	200
300	300
400	400
500	500
600	600
700	700
800	800
900	900
1000	1000
1100	1100
1200	1200
1300	1300
1400	1400
1500	1500
1600	1600
1700	1700
1800	1800
1900	1900
2000	2000
2100	2100
2200	2200
2300	2300
2400	2400
2500	2500
2600	2600
2700	2700
2800	2800
2900	2900
3000	3000
3100	3100
3200	3200
3300	3300
3400	3400
3500	3500
3600	3600
3700	3700
3800	3800
3900	3900
4000	4000
4100	4100
4200	4200
4300	4300
4400	4400
4500	4500
4600	4600
4700	4700
4800	4800
4900	4900
5000	5000

Not a part of the map published with a contour interval of 100m.
 Contour interval: 100m

The measured total magnetic force values of the survey area vary from 42,300 to 44,800 nT. General trend of magnetic changes is low in north and high in south, which is concordant with the global geomagnetic field on the earth.

(2) Magnetic Anomaly

The first order trending map was made from the total magnetic force map, and the total magnetic force anomalies were derived as the residual of total magnetic force values and the first order trending values, as shown in Fig. 3-3-2. At the same time, the residual magnetic anomaly map derived from total magnetic forces and International Geomagnetic Reference Field (IGRF) values were also made as shown in Fig. 3-3-3. Contour interval of each map is 50 nT.

When comparing residual anomaly of trending with residual anomaly of IGRF, both maps show the same pattern of anomaly but the values of anomaly on IGRF map are about 100 nT lower than those on trending map on the whole. The characteristics of magnetic anomalies from IGRF residual are as follows;

As the general magnetic trend of the survey area, NNE-SSW trending positive magnetic anomaly zone is dominant and another positive anomaly zone is also observed crossing the main anomaly zone. On this map, Vine-Mathews magnetic lineation was not clearly identified. Most of the magnetic anomalies in the survey area were in the amplitude of -300 to +300 nT, with rather much negative anomalies on the whole. More detail characteristics are as follows;

Three anomaly zones in NNE-SSW trending run through the area from north to south with a maximum amplitude of the anomaly is about +300 nT. The central positive anomaly zone runs generally along the spreading center. Positive anomaly zones on both sides run in the same distance from the central anomaly zone, and they gradually become close with the spreading center towards south. Most of the positive magnetic anomaly in the center corresponds to the topographic high due to the spreading center. While around $19^{\circ} 43'S$, $20^{\circ} 10'S$, a positive anomaly running in east to west was recognized across the positive anomaly along the spreading center. Negative magnetic anomalies on the contrary, were observed in the furrow of the overlapping spreading center in the north of the central part of the survey area, and in the deepest basin in the northern edge of the area.

In the central part of the area, around $20^{\circ} 40'S$, $176^{\circ} 00'W$, and in the southern part of the area around $21^{\circ} 55'S$, $176^{\circ} 18'W$, positive magnetic anomalies with a maximum amplitude over +250 nT were observed in wide area. The areas near those positive anomalies are characterized by distribution of large scale negative anomalies with a maximum amplitude under -400 nT.

A dipole magnetic anomaly was detected around $20^{\circ} 10'S$, $176^{\circ} 49'W$ in the southern part of the northern survey area, with an amplitude from -450 to +50 nT, and the anomaly generally locates in the flat area.

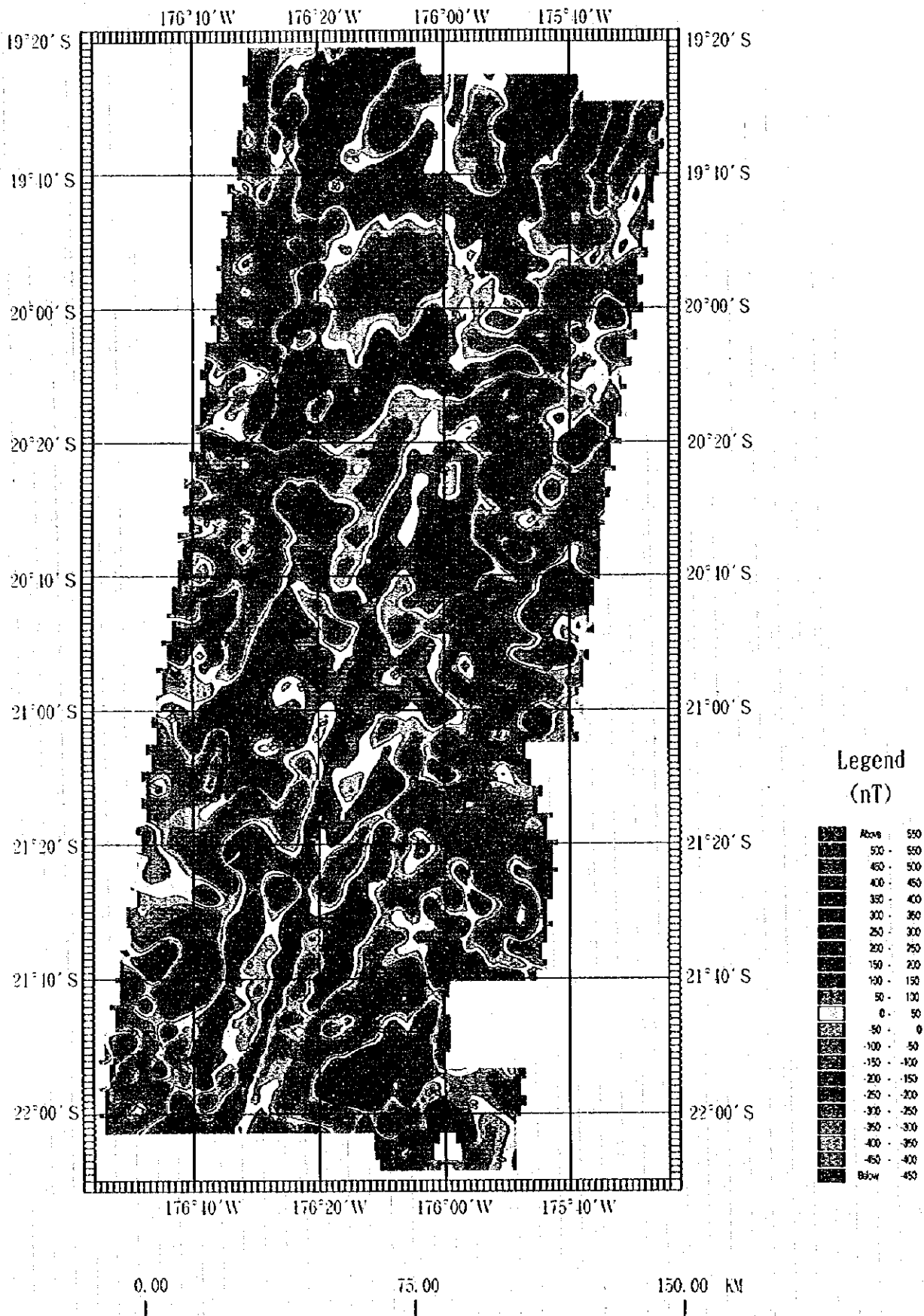


Fig. 3-3-2 Magnetic anomaly map from IGRF residual gridded with a spacing of 1.5km. Isomagnetic lines are at 50nT intervals.

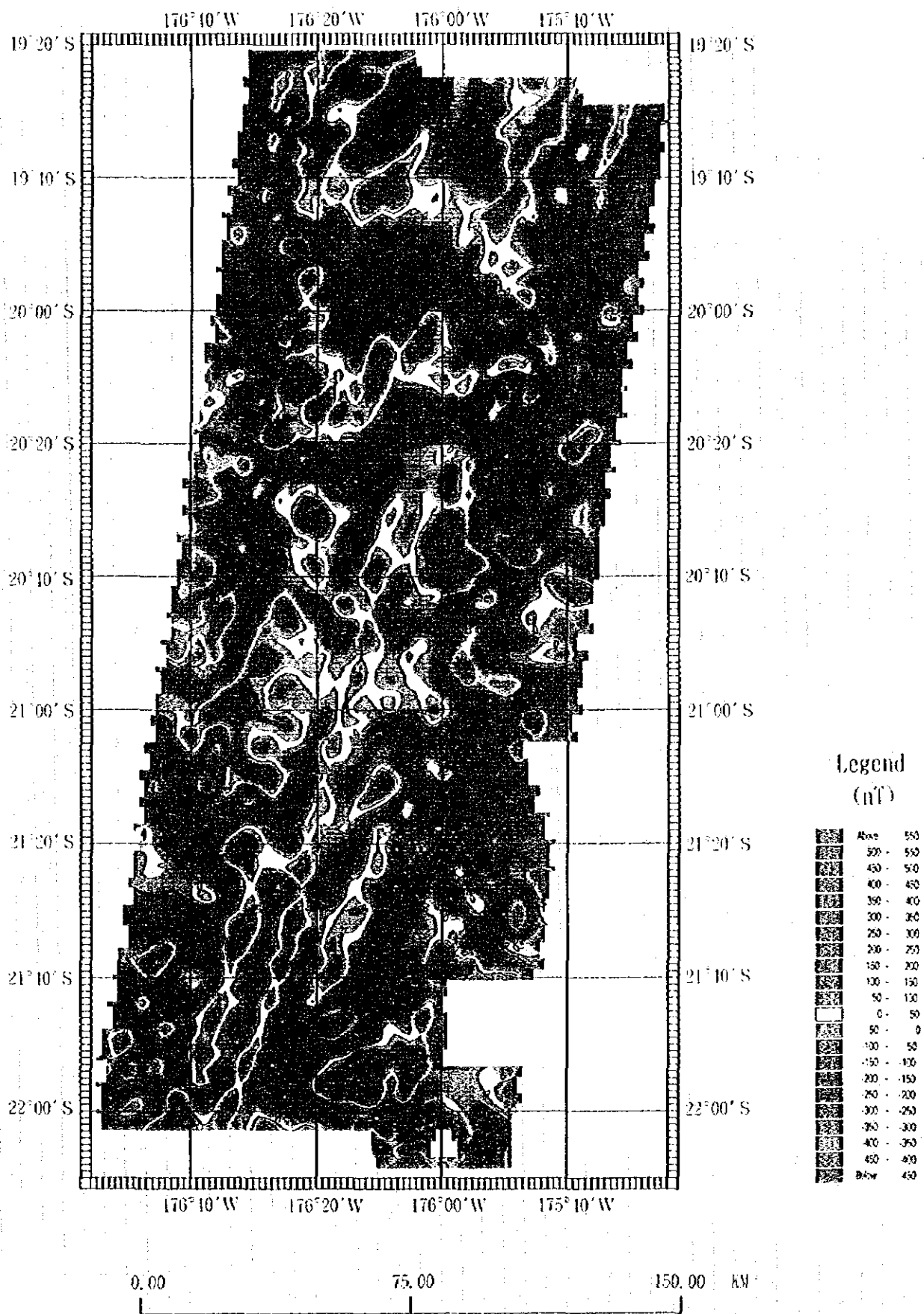
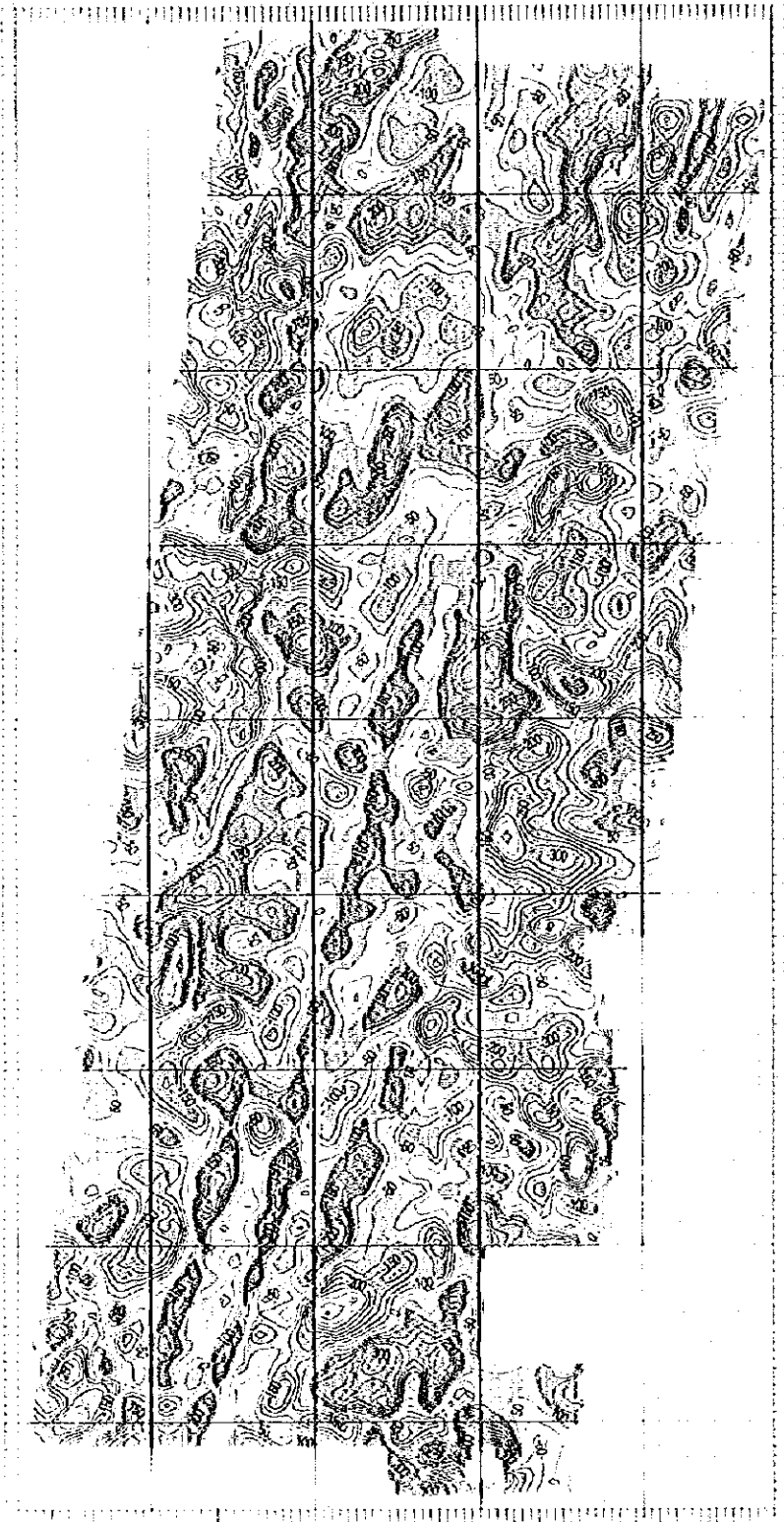
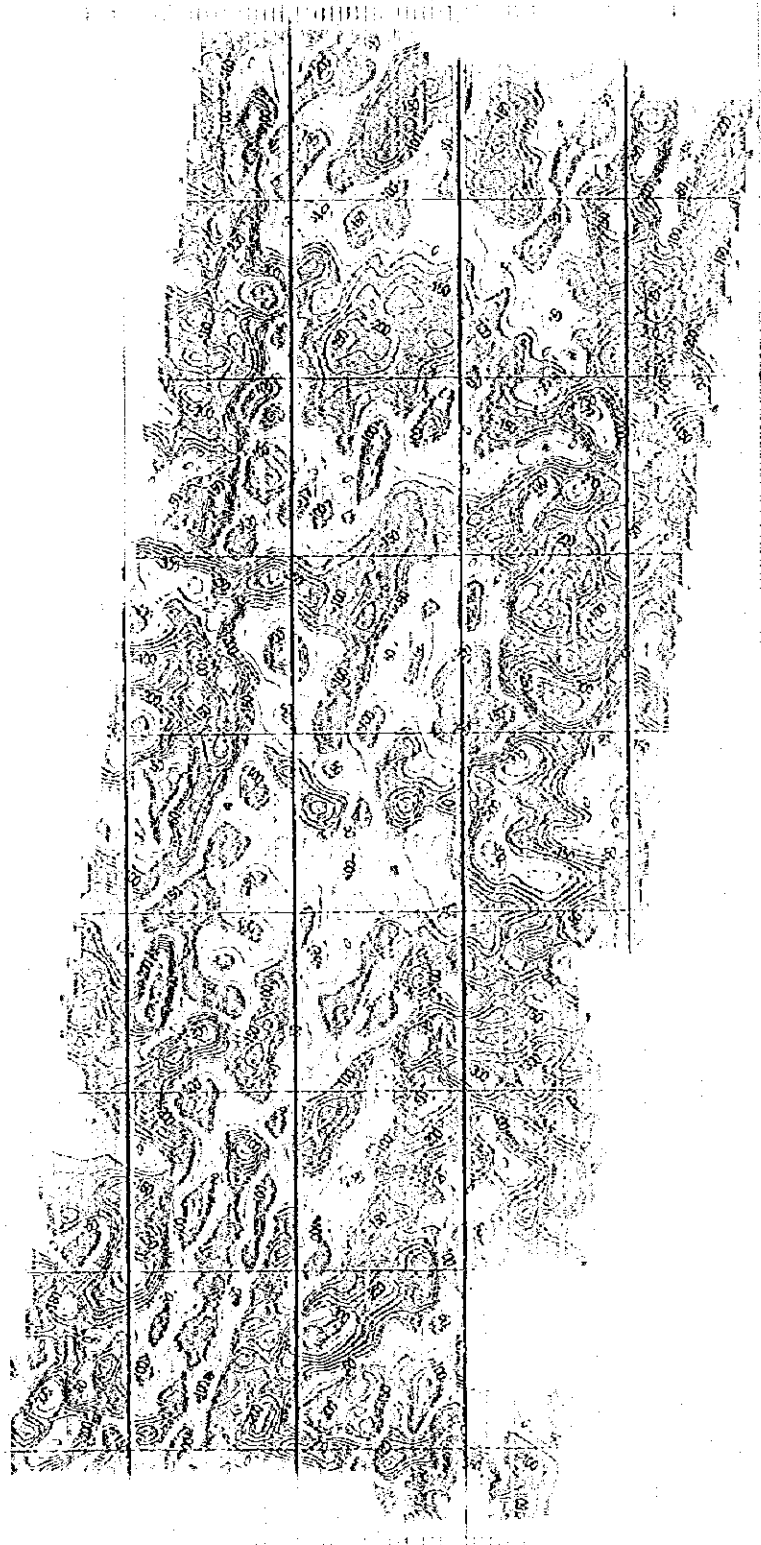


Fig. 3-3-3 Magnetic anomaly map from trend surface residual gridded with a spacing of 1.5km. Isomagnetic lines are at 50nT intervals.



1 2 3 4 5 6 7 8 9 10 11 12 13 14 15 16 17 18 19 20 21 22 23 24 25 26 27 28 29 30 31 32 33 34 35 36 37 38 39 40 41 42 43 44 45 46 47 48 49 50 51 52 53 54 55 56 57 58 59 60 61 62 63 64 65 66 67 68 69 70 71 72 73 74 75 76 77 78 79 80 81 82 83 84 85 86 87 88 89 90 91 92 93 94 95 96 97 98 99 100

1. The drawing is a technical drawing of a topographic map or a detailed architectural plan. It features a grid of vertical and horizontal lines overlaid on a dense, irregular pattern of lines and shapes. The drawing is enclosed in a double-line border.



In the southern part of the area, a typical dipole magnetic anomaly was detected. Its amplitude is -400 to +450 nT, which is the largest anomaly in the whole area. This magnetic anomaly may be due to the seamount at a water depth shallower than 500 m.

(3) Reduction-to-the-pole Anomaly

At the low-middle latitude on the Southern Hemisphere, magnetic anomaly caused by normal magnetized source is a pair of anomalies with the positive anomaly on the north side and the negative on the south side. On the other hand, magnetic anomaly caused by the same source located at the magnetic pole is a single positive anomaly just above the source. Therefore, obtained IGRF residual magnetic anomaly is transformed into a set of single anomalies by reduction-to-the-pole operation.

On a reduction-to-the-pole anomaly map, positive anomalies are distributed just above normal magnetized source. Therefore, it becomes easy to compare magnetic anomaly with topography and geology and to interpret magnetic source distribution. In the survey area, many reverse magnetized structures are detected. In this case, negative anomaly exists just above the reverse magnetized source.

In the survey area, difference of latitude between north and south edge is so large as 170 minutes, therefore difference of inclination is large too, about 5 degrees. 41 degrees which is an inclination at the central part of this area, was adopted for making reduction-to-the-pole anomaly map (Fig. 3-3-4).

The main characteristics of reduction-to-the-pole anomalies are stripes of positive and negative anomalies. Positive anomalies correspond to normal magnetized sources, while negative anomalies to reverse magnetized sources. In comparison with IGRF residual magnetic anomaly map, amplitudes of anomaly become larger, arrangement in NNE-SSW trend is emphasized and correlation with topography is recognized more clearly. Topographic high such as island margin or seamount corresponds to positive magnetic anomaly. Especially, around the ridge forming the spreading center at the central-southern part of the survey area or near the seamounts and ridges scattered in the whole area, positive anomalies are remarkable. The characteristics of reduction-to-the-pole anomalies are as follows;

Three main anomalous areas are recognized on the whole; a positive anomaly running from south to north at the center of the survey area and two negative anomalies at east and west side of the central positive anomalous area. The former corresponds to normal magnetized source, the latter to reverse magnetized source.

In the positive anomalous area, three series of positive anomaly belts are distributed intermittently in N-S direction, and most of positive anomaly belts correspond to the ridge in its position or strike. Especially, central positive anomaly belt is continuous in shape generally corresponding to the ridge. Positive anomaly belts show side stepping or skewness everywhere, especially around $20^{\circ} 00'S - 20^{\circ}$

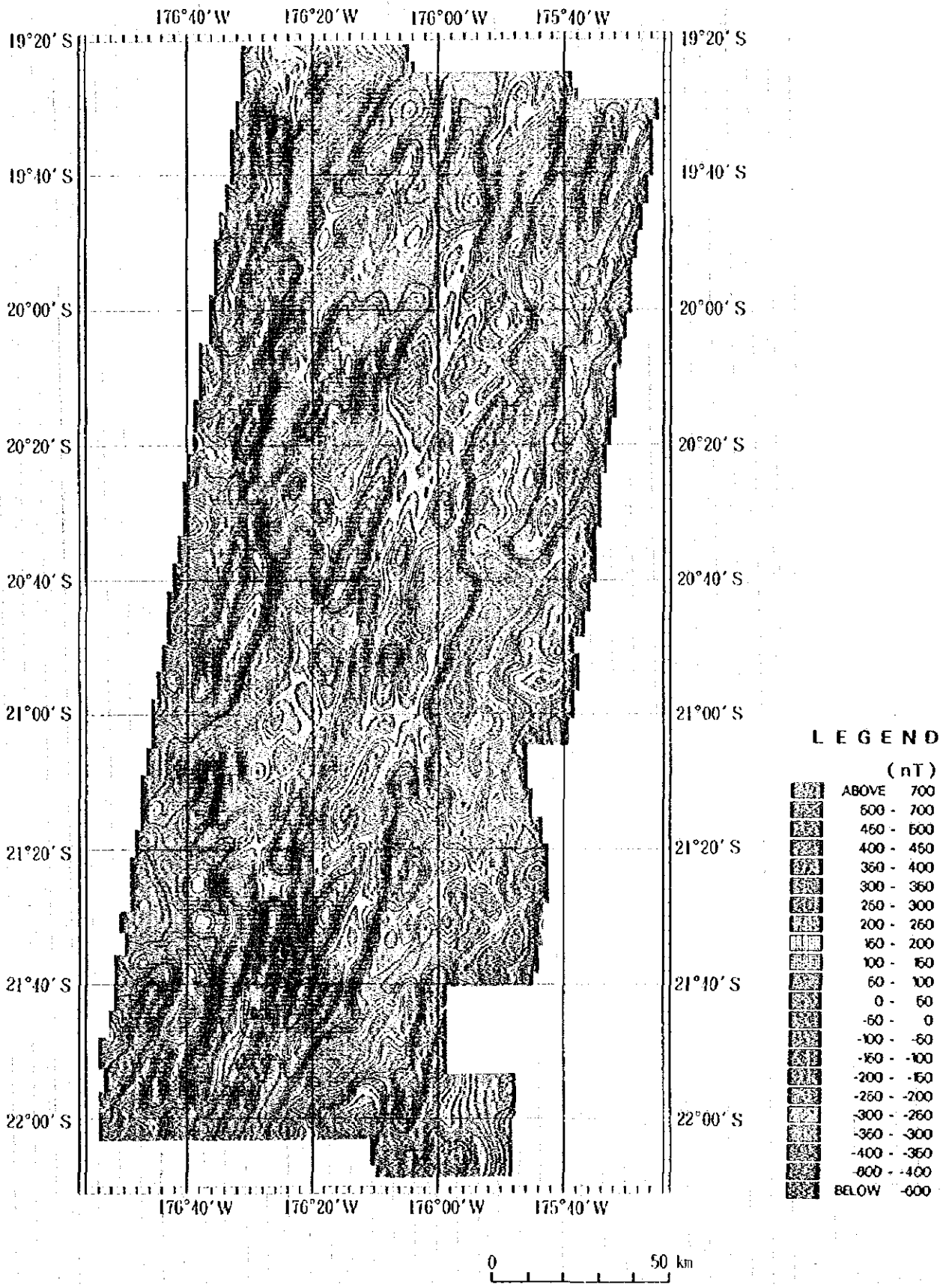


Fig. 3-3-4 Reduction-to-the-pole anomaly map.
Isomagnetic lines are at 50nT intervals.

20'S remarkably. These are considered to reflect fracture zone with E-W trend or skew structure such as overlapping spreading center.

(4) Magnetization

In the three dimensional analysis of magnetization, magnetic body beneath the sea bottom was assumed by a set of prisms and magnetization of each prism was calculated by 3-D inversion method.

Depth of upper surface of each prism was defined as the sea bottom and depth of the lower limit was set as 16 km under the sea level. Magnetization distribution map made by three dimensional analysis are shown in Fig. 3-3-5. The characteristics of magnetization distribution and correlation with topography and spreading center are summarized as follows;

① General magnetization distribution

Magnetization in the survey area varies from -3 to $+3$ A/m. The characteristics of magnetization distribution are positive and negative magnetization stripes arranged in the direction of NNE-SSW parallel with the spreading center. These magnetic stripes are estimated to have been made by spreading of the ocean crust and repeated reverse of geomagnetic field. Positive magnetization is considered to have been made by the recent geomagnetic field.

On the whole, magnetization distribution is divided into two areas, "positive magnetization dominant area" and "negative magnetization dominant area" corresponding to the positive anomalous area and the negative anomalous area on the reduction-to-the-pole anomaly map, respectively.

Especially, continuous positive magnetization dominant zone with N-S trend at the center of the survey area changes its width according to latitude; 70 km in the northern part, 50 to 60 km in the central part and 30 km in the southern part.

② Comparison with topography

The survey area locates in the basin bounded on the east and west by topographic high. In this basin, there are many large or small ridges, seamounts and grabens arranged in the direction of NNE-SSW.

In comparison with the ridges or grabens, both high and low magnetizations correspond to the topography; high magnetization zones correspond to ridges and low magnetization zones correspond to grabens in general. Especially, in the positive magnetization dominant area, several high magnetization zones running from south to north intermittently have good correlation with ridges.

On the contrary, low magnetization zone corresponding to ridge and high magnetization zone corresponding to graben are also detected in places. It means that normal magnetization and

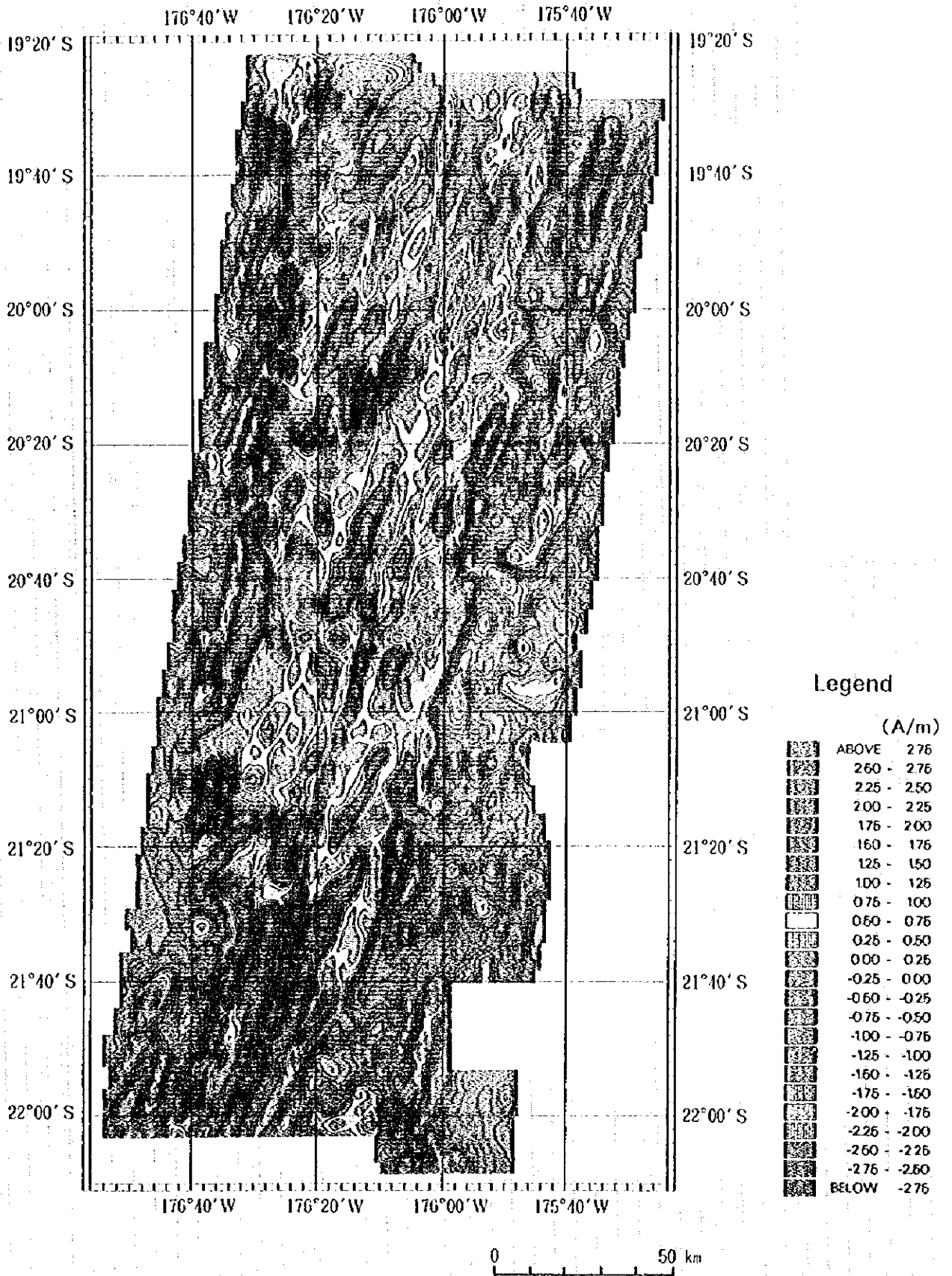


Fig. 3-3-5 Magnetization amplitude map at 0.25 A/m intervals.

reversed magnetization are mixed on the whole area.

③ Study on the spreading center

Several high anomaly belts in the positive magnetization dominant area correspond to ridges in general. Especially, high anomaly zone in the center of positive magnetization dominant area is continuous in shape and corresponds to the ridges. This ridge is considered to be the spreading center. This spreading center become to shift from center to east in the positive magnetization dominant area towards north, becoming vague in continuity in the northern part of the survey area.

Judging from the characteristics that the spreading center tends to shift eastward and the width of the positive magnetization dominant area becomes wider toward north, it is considered that spreading rate increases towards north or the age when seafloor spreading began was earlier in the northern part than in the southern part and rate of spreading in the west side of the spreading center is a little larger than in the east side.

High anomaly belts in the positive magnetization dominant area show side stepping or skewness everywhere. These skewnesses exist mainly in four areas in the vicinity of $19^{\circ} 48'S, 176^{\circ} 24'W$, $20^{\circ} 10'S, 176^{\circ} 00'W$, $20^{\circ} 24'S, 176^{\circ} 24'W$ and $21^{\circ} 14'S, 176^{\circ} 32'W$. It is estimated that there are skew structures in these areas with a possibility of EW trending fracture zone or overlapping of ridges and grabens.

(5) Magnetic Structure

In comparison with bathymetric map, magnetic structure map shown in Fig. 3-3-6 grouped as follows;

- ① high positive magnetization zone over $+1 A/m$,
- ② high negative magnetization zone under $-1 A/m$ and
- ③ boundary between positive and negative magnetization with ticks indicating the direction from positive to negative.

The characteristics of each item are as follows;

① High positive magnetization zone

High positive magnetization zones over $+1.0 A/m$ are distributed mainly in the positive magnetization dominant area, but some zones correspond to seamounts in the negative magnetization dominant area.

High positive magnetization zones in the positive magnetization area show good correlation with topographic high represented by the spreading center, but high positive magnetization zones are

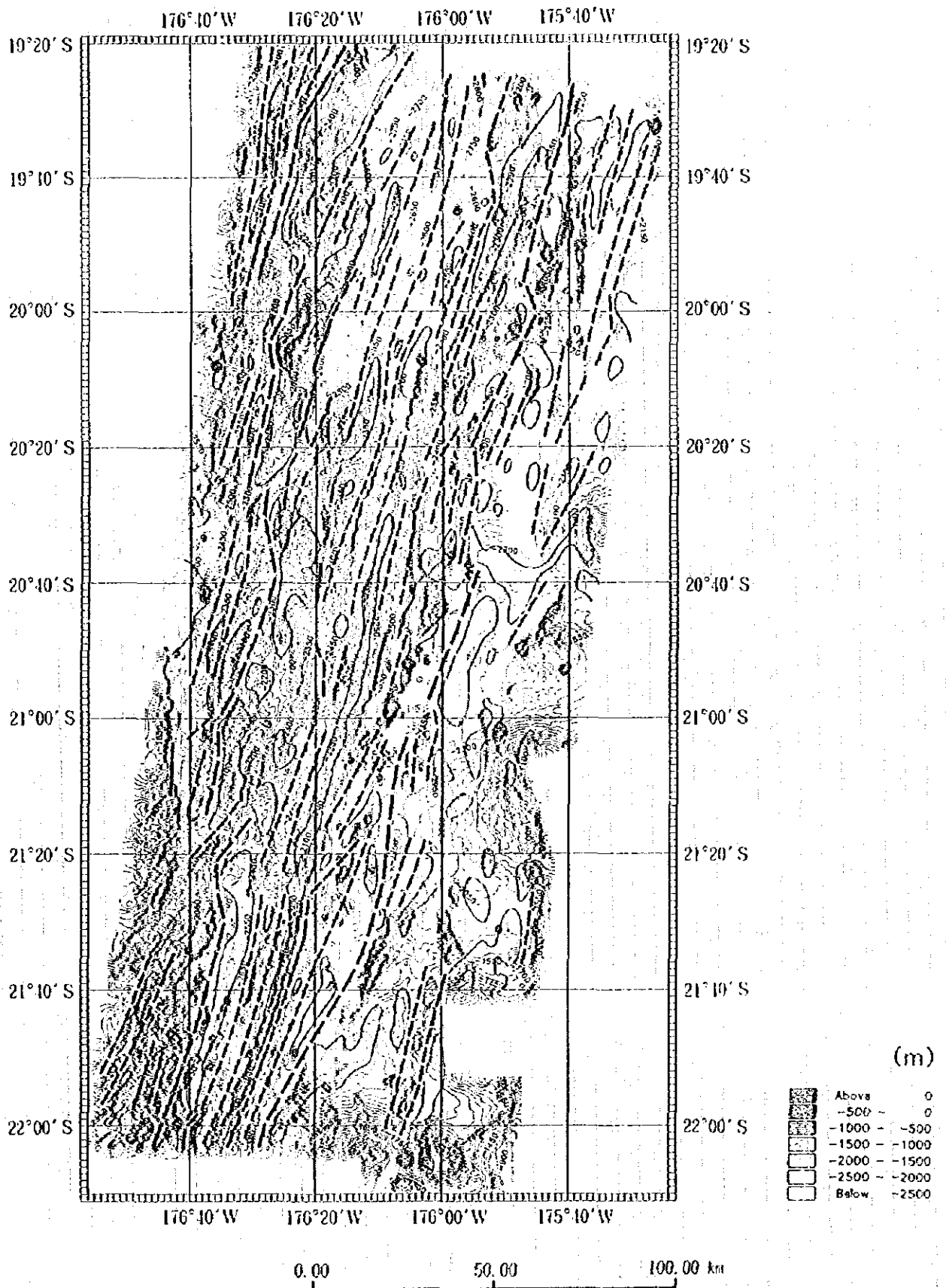


Fig. 3-3-6 Magnetic structural map. Positive and negative magnetizations greater than ± 1 A/m are shown as red and blue circular areas respectively. Dashed lines with ticks show borders between positive and negative magnetizations. Bathymetry at 50m intervals is added for reference.

Faint, illegible text at the top of the page, possibly a header or title.



also distributed at topographic low like graben in the vicinity of $21^{\circ} 40'S, 176^{\circ} 35'W$, $20^{\circ} 10'S, 176^{\circ} 06'W$, $19^{\circ} 50'S, 176^{\circ} 10'W$ and $19^{\circ} 32'S, 175^{\circ} 58'W$.

② High negative magnetization zone

High negative magnetization zones under $-1.0 A/m$ are distributed mainly in the negative magnetization dominant area, showing good correlation with topographic low. In the positive magnetization dominant area, high negative magnetization zones are distributed between the high positive magnetization zones in small scale.

Distributions of high negative magnetization zones in the negative magnetization dominant area are not so linear as high positive magnetization zones with N-S trend but widely dispersing.

③ Boundary between positive and negative magnetization

Boundaries between positive and negative magnetization zone distributed side by side are shown by fault like border line and tickes indicating the direction from positive to negative. Especially, boundary between positive and negative magnetization dominant areas are emphasized by thick lines.

The border lines are running intermittently in the direction of NNE-SSW. In the positive magnetization dominant area, many border lines from several kilometers to over 20 km wide are detected. However, in the negative magnetization dominant area, such border lines are not seen so many. Continuities of border lines are broken everywhere in the survey area. In the northern part near $20^{\circ} 00'S - 20^{\circ} 20'S$, reverse of continuity of positive and negative magnetization are detected in places.

3-4 Geological Structure

(1) Geological Structure

Lineament map made from the bathymetric map is shown in Fig. 3-4-1, in which the location of the spreading axis was assumed by topographic features and high sound amplitude in the MBES acoustic reflection image. In this chapter and hereafter, the spreading axis or the spreading center in the survey area corresponds to the above mentioned one.

The main trend of lineaments in the survey area is NNE-SSW in parallel with the spreading axis. (This direction is also parallel with the Tonga Trench and the Tonga Ridge.) Most of lineaments indicate the fault cliff formed by the normal fault movement accompanied by the spreading of the oceanic crust. In the western part of the area, there are lineaments running in N-S to NNW-SSE. In the eastern part of the area, there are also NE-SW trending lineaments oblique to the spreading axis in low angle.

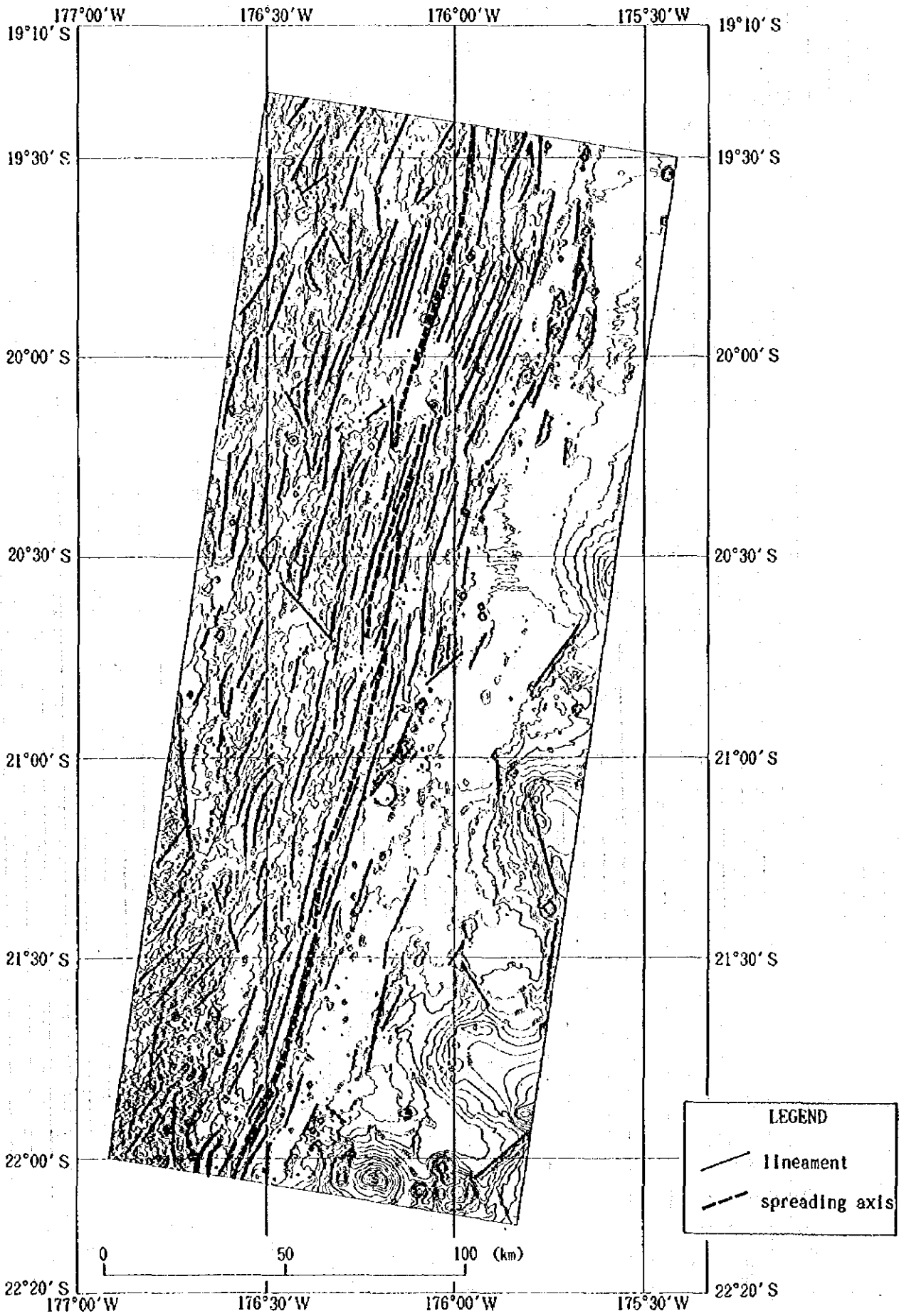


Fig. 3-4-1 Lineament map

Geological structure map is shown in Fig. 3-4-2, in which the main and the most distinctive geological structure is the spreading axis of the Lau Basin running in NNE-SSW direction in the area. This spreading axis consists of several grabens and ridges in echelon form. Overlapping spreading center is seen in the central part of the survey area. The lineaments around the overlapping spreading center and its bending zone are developed in parallel with the trend of the spreading center.

In the northern half of the survey area, the spreading center mainly forms the grabens, and newly borne ocean crust is seen in about 25 to 35 km in width. While in the southern half of the area, the spreading center mainly forms the ridges, and these ridges, formed by volcanic activity resulted from spreading, have the width of about 10 km. The difference of spreading center in formation between both areas is described to the starting age of spreading, spreading rate, lithology of volcanic and so on.

In 10 to 40 km east of the spreading axis, knoll chains lie in parallel with the spreading center, which were formed by eruptions along the fracture zone parallel with spreading center. In the area from the eastern edge to the southeastern part of the area, there is active submarine volcano range which corresponds to the volcanic front (Tofua Volcanic Arc) of the Tonga Ridge.

As mentioned above, the survey area can be divided into two main areas, however, based on the geological structure around the spreading center, the survey area is classified in detail into five tectonic segments (TS-A to TS-E). These classified zones are also shown in Fig. 3-4-2.

1) Tectonic segment TS-A

Location : North of $19^{\circ} 44'S$, northernmost part of the survey area

Topography : The spreading center forms a ridge in the south and a graben in the north. There is a small basin in the northern edge of the area, and the spreading center which runs through the survey area disappears in this basin.

Structure : Near the spreading center, no eminent east-west symmetric structure like tectonic segment TS-B is seen. The trend of the spreading center in the northern part of the area is north-south, and in the southern part it shows NNE-SSW. In this surrounding area, however, the trend of the geological structure is NNE-SSW in the northern area and north-south in the southern area. As a result, both structures cross each other in two areas. We presume that both structures were originally in parallel each other and the stress field being changed with the progress of spreading, the spreading center propagated to the south and shifted towards the east.

Several small basins exist in the western side of the spreading center. These basins could be the dead spreading center. On the basis of this assumption, the spreading center in this segment could successively move from the west to the east.

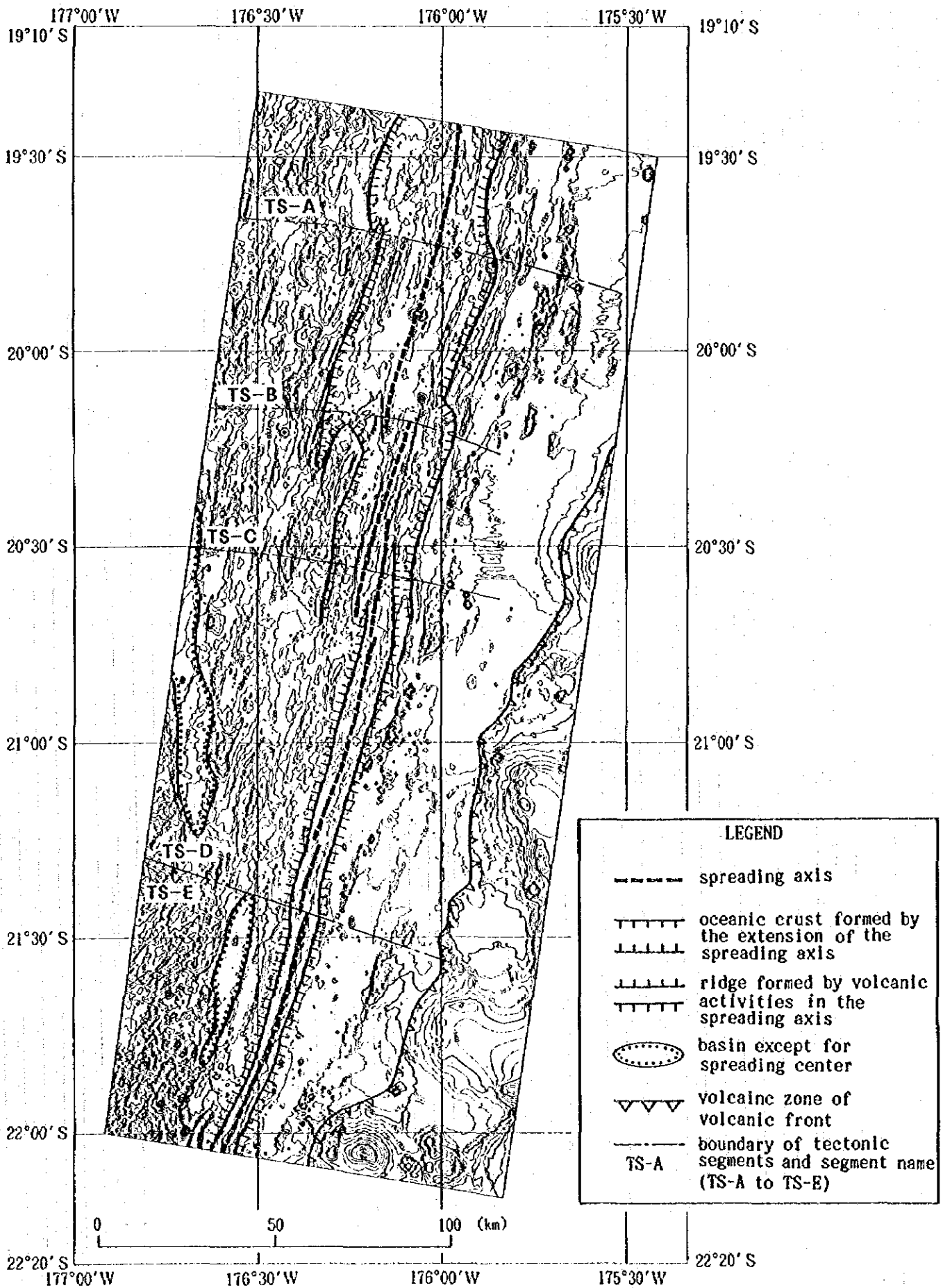


Fig. 3-4-2 Geological structure map

2) Tectonic segment TS-B

Location : From about $19^{\circ} 44'S$ to about $20^{\circ} 10'S$

Topography : The spreading center forms a graben. Within about 35 km in width from the spreading center as its center, grabens and horsts alternately exist showing east-west symmetric form. Nearby $19^{\circ} 54'S$, two semicircular shaped knolls exist separating by the spreading center. Around 35 km in the east of the spreading center, NNE-SSW trending knoll chain exists.

Structure : A strike of the spreading axis is $N20^{\circ} E$ to $N25^{\circ} E$ and NNE-SSW trending lineaments develop in parallel with the axis. Most of these lineaments correspond to the boundary of horst and graben, and these boundaries show normal faults caused by tension field due to the spreading. Maximum length of the fault cliff rises up to 45 km. In the southern part of the area, fault cliffs are not so clear.

In the southernmost part of the spreading center, the strike of the center changes to north-south disappearing its continuity towards the south. While in the eastern side, there is the northern edge of another spreading center in tectonic segment TS-C. Around $20^{\circ} 10'S$, two spreading centers overlap each other forming an overlapping spreading center.

3) Tectonic segment TS-C

Location : From about $20^{\circ} 10'S$ to about $20^{\circ} 33'S$

Topography : The spreading center shows a graben of 2 to 4 km in width. In the central part of the graben, topographic high features such as a chain of small hills and a horst are seen. In this surrounding area of the spreading center, parallel trending graben and horst are seen alternately.

Structure : A strike of the spreading axis is about $N20^{\circ} E$ and in the southern end it shifts to $N10^{\circ} E$. Lineaments develop in parallel with the axis, corresponding to normal faults at the boundary of horst and graben.

In the southern end of the spreading center, the strike of the spreading center changes to north-south disappearing its continuity towards the south. While in the eastern side, there is the northern edge of another spreading center in tectonic segment TS-D. The strike of this spreading center in TS-D is north-south, and it is contacted with the middle part of the spreading center in TS-C. Near $20^{\circ} 25'$ to $20^{\circ} 33'S$, two spreading centers overlap each other forming an overlapping spreading center. Therefore, the spreading center in this segment forms the overlapping spreading center at the north and south end.

4) Tectonic segment TS-D

Location : From about $20^{\circ} 33'S$ to about $21^{\circ} 27'S$

Topography : The spreading center generally forms a ridge. The detail topography of its summit shows a ridge in the northern and southern part of the area, but a graben in the center of the area. In more detail, ridges and grabens being the spreading center show the echelon. In 5 to 15 km east of the spreading center, several knoll chains exist in NNE-SSW to NE-SW direction.

Structure : A strike of spreading axis is $N20$ to $10^{\circ} E$ in echelon shape. The ridge formed by the present spreading center has a width of about 10 km. No obvious group of parallel faults is recognized along this ridge. Most of lineaments are in parallel with the spreading center. Curve shaped lineaments are recognized in the western part.

5) Tectonic segment TS-E

Location : Southern side of $21^{\circ} 27'S$, southern end of the survey area.

Topography : The spreading center forms a ridge, whose width is about 6 km and relative height 500 to 600 m. The character of this ridge is a big relative height and a steep slope in comparison with the ridges and horsts in other areas. These topographic features are typically seen also at the knoll chain. These characters are caused by lava properties (such as viscosity, form, etc.) and the quantity of the eruption.

The submarine volcanoes on the volcanic front are seen about 25 km east of the spreading center in the southern end of the area. This part is the place where the distance between the spreading center and the volcanic front is the shortest in the survey area. In the western area (southwest of the survey area), many knolls form a seamount, but no array distribution is recognized.

Structure : A strike of the spreading axis is $N15^{\circ} E$ in the north, and $N25^{\circ} E$ in the south. The obvious bending point of the strike exists near $21^{\circ} 49'S$. The lineaments parallel with the spreading center are seen only close to the axis. While in the western area, NE-SW trending lineaments are dominant.

(2) MBES Acoustic Reflection Image

With the object of understanding bottom sediments and outcrop of exposures of the rock, especially due to outcrop rock accompanied by spreading rift, and distribution of sediments near the outcrop, the MBES acoustic reflection image (Fig. 3-4-3) has been made by receiving acoustic pulses from each beam. In this image, dark part corresponds to high sound amplitude from the bottom, and light corresponds to low sound amplitude. On this aspect, MBES acoustic reflection image can be separated into three groups;

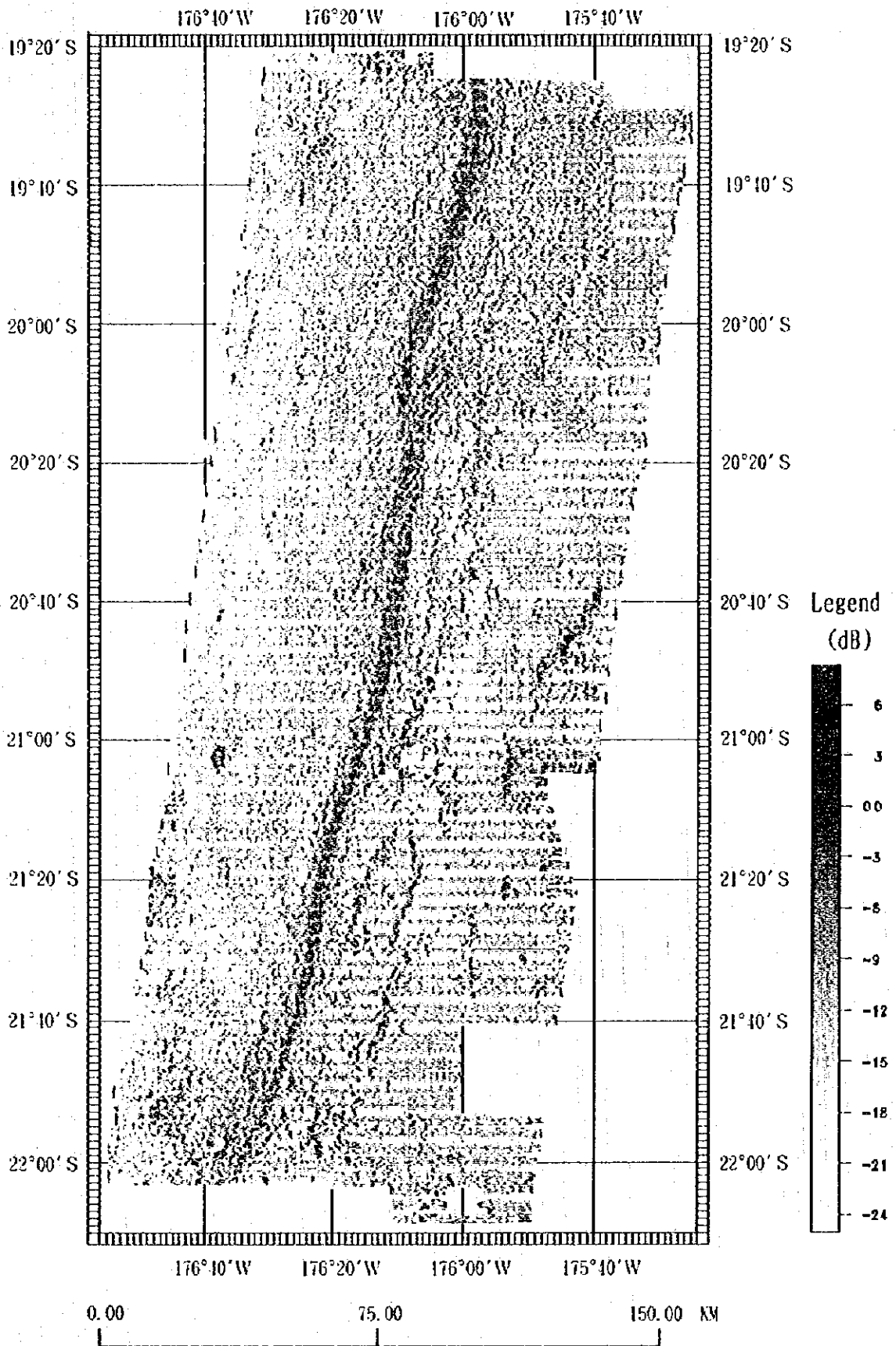


Fig. 3-4-3 Acoustic reflection image based on MBES. Darkly shaded areas indicate high sound amplitudes and light areas indicate low sound amplitudes.

